DEPARTMENT OF PHYSICS

WASHINGTON STATE UNIVERSITY

PULLMAN, WA 99164-2814

REPORT NUMBER N00014-85-C-0141-AR6

ANNUAL SUMMARY REPORT NO. 6

OCTOBER, 1986

RESEARCH ON ACOUSTICAL SCATTERING, DIFFRACTION CATASTROPHES, OPTICS OF BUBBLES, PHOTOACOUSTICS, AND ACOUSTICAL PHASE CONJUGATION

by

Philip L. Marston

Prepared for:

OFFICE OF NAVAL RESEARCH

PHYSICS DIVISION (CODE 1112)

CONTRACT NO. N00014-85-C-0141

TABLE OF CONTENTS

I. External Communications Supported by this Contract (since October 1, 1985):

A. Papers Published in Refereed Journals:

1. P. L. Marston, "Cusp diffraction catastrophe from spheroids: generalized rainbows and inverse scattering," Optics Letters 10, 588-590 (1985).
2. K. L. Williams and P. L. Marston, "Synthesis of backscattering from an elastic sphere using the Sommerfeld-Watson transformation and giving a Fabry-Perot analysis of resonances," Journal of the Acoustical Society of America 79, 1702-1708 (1986).

B. Papers Submitted to Refereed Journals:

1. P. L. Marston, "Transverse cusp diffraction catastrophes: some pertinent wavefronts and a Pearcey approximation to the wavefield," Journal of the Acoustical Society of America (submitted).

C. Books (and sections thereof) Published: (Note--these items were typically subject to review by committee or by a topical editor):

1. P. L. Marston, "Directional caustics in acoustics and in light scattered from bubbles," in Proceedings of the 12th International Congress on Acoustics (Beauregard Press, Toronto Canada, 1986), pp. I1-1.1, 1.2.
2. K. L. Williams and P. L. Marston, "Scattering from an aluminum sphere: Fabry-Perot analysis of resonances based on the Watson transformation," Proceedings of the 12 International Congress on Acoustics (Beauregard Press, Toronto Canada, 1986), pp. I1-2.1,2.2.
3. P. L. Marston and B. T. Unger, "Rapid Cavitation Induced by the Reflection of Shock Waves" in Shock Waves in Condensed Matter, Y. M. Gupta, editor (Plenum, New York, 1986), pp. 401-405.

D. Books (and sections thereof) Submitted for Publication:

1. P. L. Marston and D. S. Langley, "Bubbles in Liquid ^{4}He and ^{3}He: Mie and Physical-Optics Models of Light Scattering, and Quantum Tunneling and Spinodal Models of Nucleation," in Near Zero: New Frontiers in Physics, edited by B. S. Deaver, C. W. F. Everitt, and P. F. Michelson (Freeman, San Francisco, to be published in 1986 or 1987), accepted for publication.

E. Invited Presentations at Topical or Scientific/Technical Society Conferences:

1. P. L. Marston and K. L. Williams, "Rayleigh waves on an elastic sphere: Theory and experiment," Invited paper presented by P. L. Marston at the 22nd Annual Meeting of the Society of Engineering Science (Penn. State Univ., October 1985).

F. Abstracts of Papers (presented at meetings) Containing Significant Information Not Yet Published (or submitted for publication) in Final Form:

1. B. T. Unger and P. L. Marston, "Optically stimulated sound from gas bubbles in water: radiation pressure and resonance response," J. Opt. Soc. Am. A2(13), P6 (1985).
2. D. S. Langley and P. L. Marston, "Forward optical glory of bubbles in liquids: theory and observations," J. Opt. Soc. Am. A2 (13), P60 (1985).

G. Reports Issued:

1. P. L. Marston, Annual Summary Report No. 5: Research on Acoustical Scattering, Optics of Bubbles, Diffraction Catastrophes, and Laser Generation of Sound by Bubbles, Accession Number AD-A161333

(Defense Technical Information Center, Alexandria, VA, issued September, 1985).

H. Dissertation Supported in Part by this Contract (to be issued to DTIC as a Technical Report):

1. S. C. Billette, "Computational Analysis of the Effects of Surface Films on the Optical Scattering Properties of Bubbles in Water" (Physics Department, M.S. Thesis, Washington State University, August 1986).

II. Preface; Explanation of Citation System Used for References; and List of Graduate Students Supported:

This report summarizes progress in research supported by the contract titled: "Propagation and Effects of Acoustical and Optical Waves." The emphasis of the report is on progress subsequent to that described in the previous Annual Summary Report, item G1 in the preceding list of "External Communications." However, for continuity, certain research items discussed there will also be mentioned. The principal sections (indicated by different Roman numerals) may be read independently of each other.

The following reference system is used in this report. References to recent external communications supported by this contract will be made by giving the section letter and number of the list given in Sec. I of the present report. For example, the first item listed in Sec. I is referenced as [A1]. Reference to other literature, including earlier work supported by this contract, are listed in Sec. IX. The first item in that list is referenced as [1].

The following students were supported either entirely or in part by contract during the period October 1, 1985 - September 30, 1986.

1. William Pat Arnott
2. Stuart C. Billette
3. Steven G. Kargl
4. Bruce T. Unger

III. Acoustical Scattering Theory and Experiments

A. Motivation for this Research: An Overview.

The general motivation for research into acoustic scattering from elastic objects of simple shape has been discussed previously.[1,2,G1] It may be thought that scattering from elastic spheres is too specialized of problem to be of any practical consequence; however, we intend to show that our understanding of the surface-wave contributions to directional caustics, which we have studied for spheres, is helpful for understanding the echoes from complicated elastic structures. The experiments on the backscattering of sound from elastic hemispheres in water (Sec. IIIE below) is a clear step in that direction. Previous work on the directional caustics in the scattering from elastic sphere was concerned with solid spheres whereas the emphasis of the current experiments is on hollow (air-filled) elastic spheres. In all cases the surrounding medium is water.

One important aspect of our research is our ability to model and measure scattering amplitudes not just in the exact backward direction but also in near backward directions since the width of the diffraction lobes in near-backward directions are indicative of the target's size.[3-5,G1]

B. Fabry-Perot Analysis of Resonances Based on the Watson Transformation and the Synthesis of Backscattering Amplitudes

This work was largely carried out by Kevin L. Williams during the course of his Ph.D. dissertation project.[5] (Since September 1985 Williams has been working in acoustics at the Naval Coastal Systems Center.) During the present contract period, two manuscripts were completed and published on this work.[A2,C2] Item C2 has been reproduced in the present report as Appendix I since it gives both an overview and the principal mathematical results. The resulting form for resonance contributions is closer to a form appearing in the analysis of Fabry-Perot resonators than to expressions appearing in Resonance Scattering Theory (RST). Unlike RST, the contributions to the scattering from

a given class of surface waves are summed directly in a way which is uniform in dependence on frequency.

Reference A2 also gives (and verifies) novel expressions for a coupling coefficient descriptive of the interaction of an acoustic wave in water with an elastic surface wave on a solid spherical surface. This type of coefficient is needed for proper extension of the Geometrical Theory of Diffraction (GTD), the prediction of scattering amplitudes from curved elastic structures in water.

C. Focused Backscattering due to Lamb Waves on Hollow Spherical Shells

Our previous quantitative analysis[4-6,A2,C2,G1] of focused backscattering due to elastic surface waves emphasized the case of a solid elastic sphere. The phenomena should also occur in the scattering of high-frequency sound from a spherical shell in water. That this is so may be seen by applying the ray diagram (Fig. 1 of Appendix I) in the case of elastic surface waves on a shell commonly known as "Lamb waves." The backward directed wavefront appears to come from a ring-like source of radius $b_l = a \sin\theta_l$ (denoted by b_R in the figure) where θ_l is the local angle of incidence at the trace velocity matching condition[A2]

$$c/c_l = \sin\theta_l, \tag{1}$$

where c is the sound speed in water and c_l is the phase velocity of the Lamb wave of interest.

Steve Kargl has carried out several experiments which clearly indicate a surface-wave construction (of large amplitude) is focused in backscattering from hollow spherical shells in water. Kargl is also working to classify these surface wave contributions by numerical solution of the appropriate characteristic equation for Lamb waves on a curved shell. These projects constitute the subject of an M.S. degree project for Kargl. Most experiments are being done with a shell made of type 440C Stainless Steel with an outer

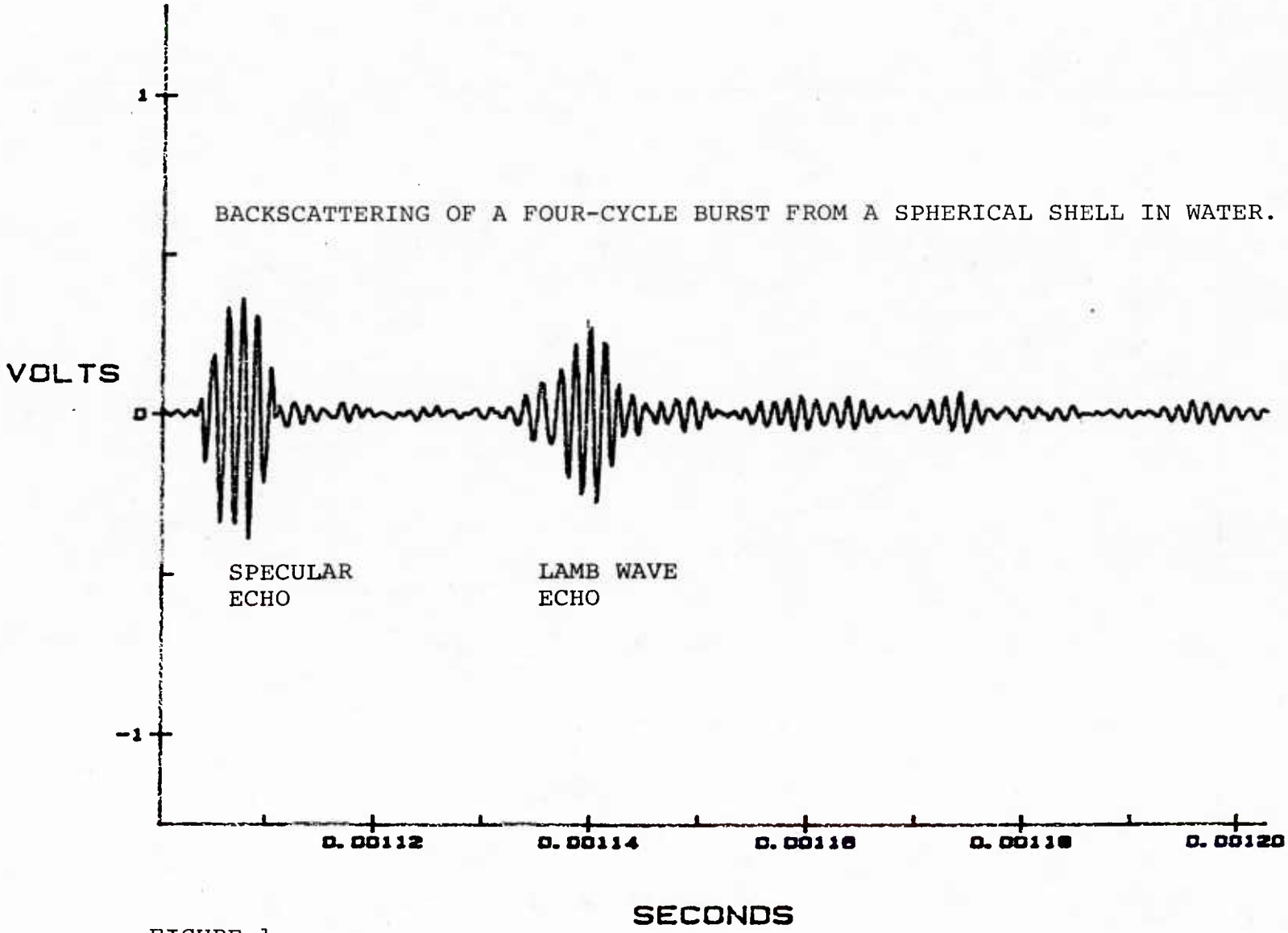
BACKSCATTERING OF A FOUR-CYCLE BURST FROM A SPHERICAL SHELL IN WATER.
VOLTS
1
0
-1
SPECULAR ECHO
LAMB WAVE ECHO
0.00112
0.00114
0.00116
0.00118
0.00120
SECONDS

FIGURE 1.

AXIAL FOCUSING OF A SURFACE WAVE

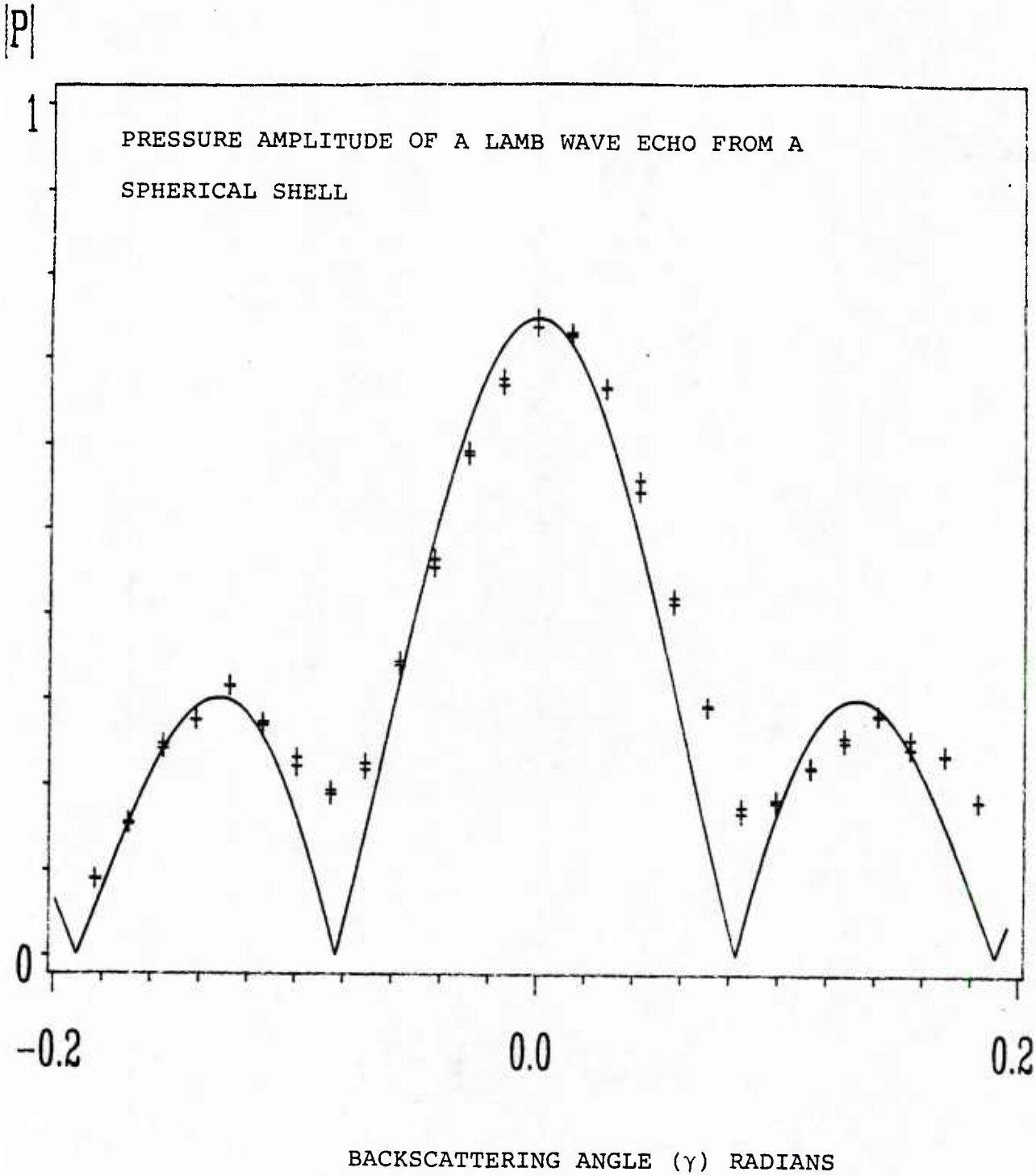

FIGURE 2.

radius a = 1.905 cm and a wall thickness of 3.1 mm. (The sphere was originally manufactured by electrowelding together two identical hemispheres so as to produce a homogenous bond at the weld. The time records of the backscattering do not depend on the orientation of the bond.) The incident wave is a sine wave having a typical duration of four cycles and a frequency f in the range 400-900 kHz.

Figure 1 is a record of the exact backward scattering for the case f = 751 kHz. The burst or echo near the left-hand side is the specular reflection from the sphere. The burst just left of center is the dominant surface wave contribution at this frequency. Note that ka = 61 where $k = 2\pi f/c$. Examination of record for the late times shows that this Lamb wave contribution is more rapidly damped than the Rayleigh wave contribution was in previous experiments[3,6] with solid elastic spheres. The relative Lamb wave/specular amplitude ratio may be greater for hollow sphere than the Rayleigh/specular ratio[6] was in the experiments with solid spheres.

Figure 2 shows the amplitude (in arbitrary units) of the earliest Lamb wave echo (i.e., the second burst in Fig. 1). The horizontal axis is the backscattering angle γ of the hydrophone receiver which is relative to the sphere's center C and a line from C to the distant sound source. The narrow central lobe and side lobe structure in Fig. 2 are manifestations of axial focusing.

In our previous experiments with solid elastic spheres[4,6] the angular dependence of the surface wave echo is of the form:

$$f_l(\gamma) \propto J_O(\lambda_l \gamma), \tag{2}$$

where the parameter λ_l gives the location (in the complex plane) of certain poles.[A2,6] The rate of radiation damping of the elastic surface wave is proportional to $\mathrm{Im}(\lambda_l)$ where in the previous cases $\mathrm{Im}(\lambda_l) << \mathrm{Re}(\lambda_l)$ and $\mathrm{Im}(\lambda_l)$ could be neglected in the evaluation of (2) so that

$$f_l(\gamma) \propto J_O(A\gamma), \tag{3}$$

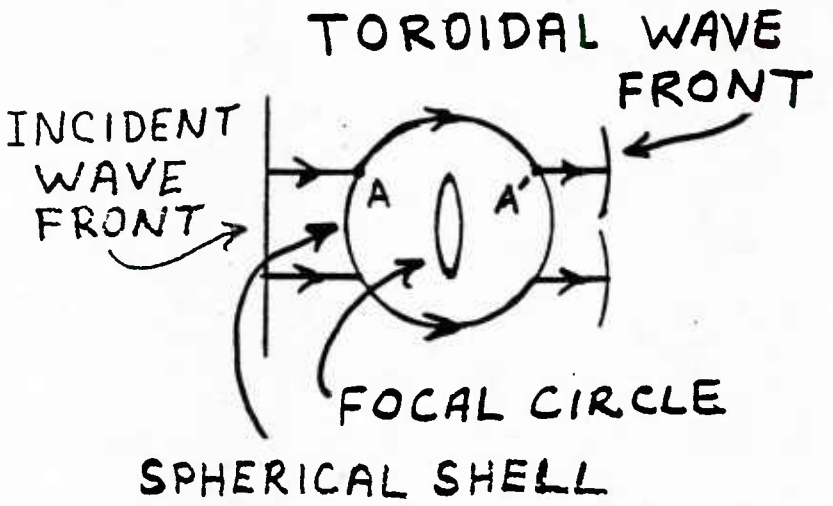

FIGURE 3(a)

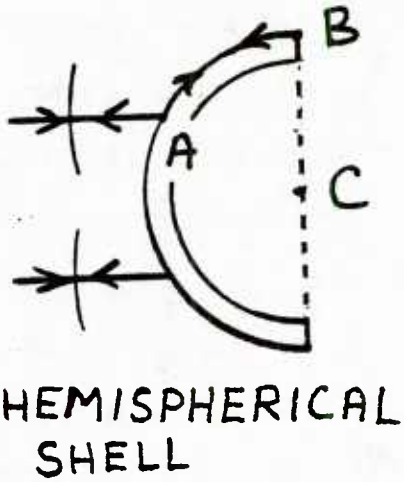

FIGURE 3(b).

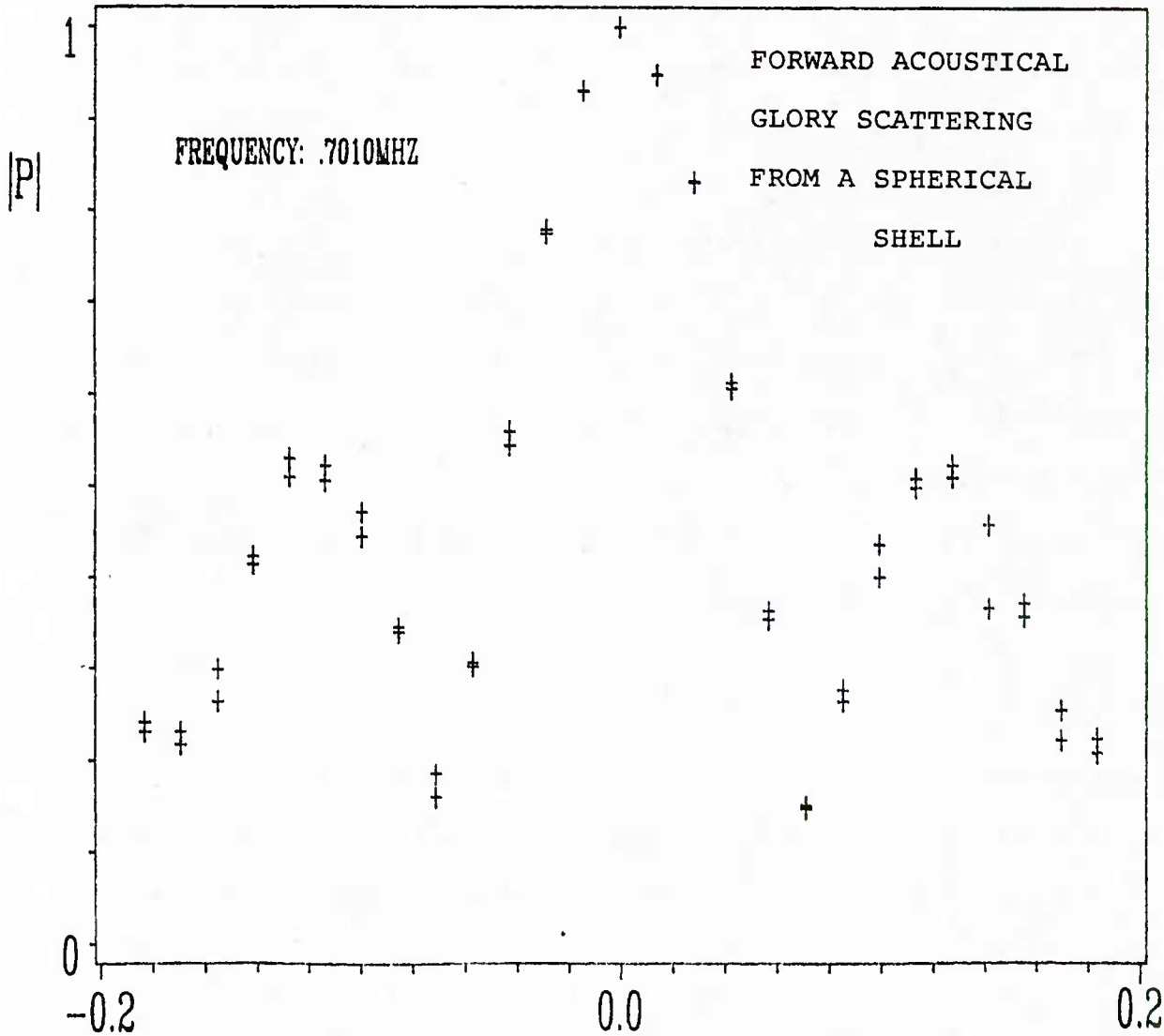

FIGURE 4. FORWARD SCATTERING ANGLE (θ) RADIANS

where $A = \mathrm{Re}(\lambda_l)$. The solid curve in Fig. 2 is an attempt to use the same approximation to fit the data by adjusting the parameter A to give a best-fit to the peaks. Unlike the previous plots for solid spheres,[4] clear discrepancies are evident close to the minima. The cause of this is evidently that we can no longer set $\mathrm{Im}(\lambda_l) = 0$ when evaluating the right-hand side of Eq. (2). This is the result of the largeness of the radiation damping of the Lamb waves. The physical reason is that the outgoing toroidal wavefront (see Appendix I) is no longer homogeneous but has an amplitude which depends on direction.

The mathematical analysis needed to improve the approximation of $J_O(\lambda_l\gamma)$ has been carried out; however, a full test of the theory will require numerical evaluation of λ_l from a characteristic equation for the shell problem. To facilitate this Kargl has recently improved the numerical method we use for finding complex roots.

D. Focused Forward Scattering due to Lamb Waves on a Hollow Spherical Shell: A Forward Acoustical Glory

In addition to backward-directed toroidal wavefronts, surface waves should also produce forward-directed toroidal wavefronts.[1] Figure 3(a) shows the ray diagram for the forward directed wavefront. The resulting amplitude should be focused along the forward axis, and, hence give rise to a forward glory. (Aspects of the optical forward glory have been studied for drops[7] and bubbles.[8]) Kargl has verified that the dominant surface-wave contribution is focused along the forward axis. Figure 4 shows the normalized amplitude of the earliest surface-wave contribution for the hollow elastic sphere discussed in Sec. IIC. For these data f = 701 kHz so that ka = 56. The narrow peak centered on forward (or 0 deg.) scattering is seen; however, a full theoretical description requires the completion of the analysis discussed in Sec. IIC. It is noteworthy that this surface wave contribution clearly precedes in time all other acoustical signals (such as geometric reflection and ordinary forward diffraction). Hence the focusing mechanism manifested in Fig. 4 is clearly different from that which causes "Poisson's spot" in the nearfield scattering.[9]

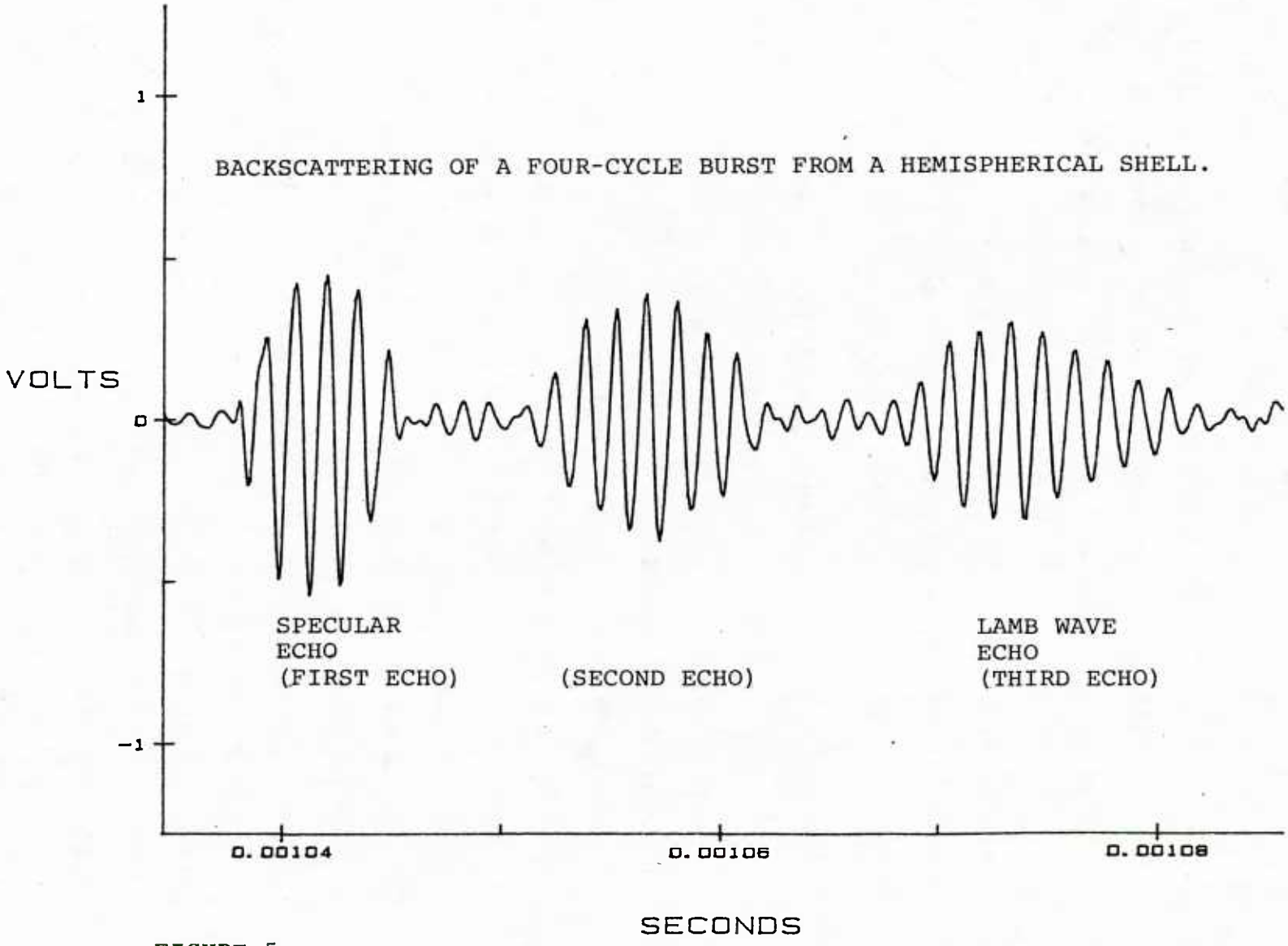
BACKSCATTERING OF A FOUR-CYCLE BURST FROM A HEMISPHERICAL SHELL.
VOLTS
1
0
-1
SPECULAR
ECHO
(FIRST ECHO)
(SECOND ECHO)
LAMB WAVE
ECHO
(THIRD ECHO)
0.00104
0.00106
0.00108
SECONDS

FIGURE 5.

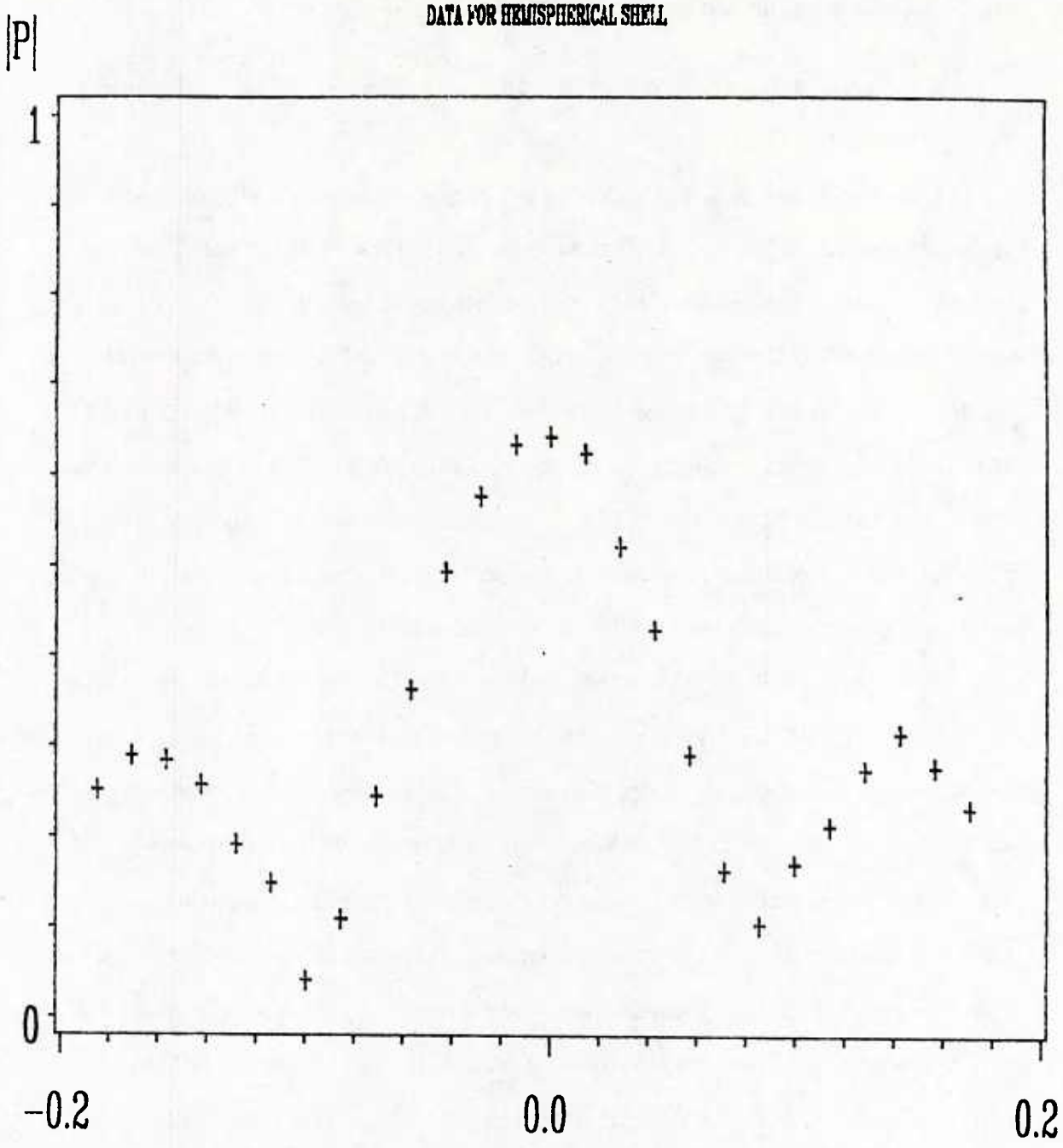
AXIAL FOCUSING OF A SURFACE WAVE
DATA FOR HEMISPHERICAL SHELL
|P|
1
0
-0.2
0.0
0.2
BACKSCATTERING ANGLE (γ) RADIANS

FIGURE 6.

Furthermore, since the sphere is hollow, this early echo must be due to a Lamb wave since no bulk waves are transmitted through the sphere.

E. Focused Backscattering Due to Lamb Waves on a Hemispherical Shell

It may be argued that (i) hemispheres will produce axially-focused scattering and (ii) that the focusing axis will depend on the angle ψ between the figure axis (of the hemisphere) and the propagation direction of the incident wave.[1] In the present discussion we will consider only the case where the angle $\psi = 0$. Figure 3(b) shows the resulting ray diagram for the case of a hemispherical shell in water. A Lamb wave is launched in the shell at point A according to the trace velocity condition, Eq. (1). When that wave reaches the free edge of the shell at B, there will be a partial reflection of the Lamb wave as well as some radiation of sound into the surrounding water. The reflected energy in the shell will not all be in the same Lamb mode as that of the incident Lamb mode.[10]

To test these ideas a spherical shell identical to the one used in the aforementioned experiments (Sec. IIIC and D) was cut along a diameter so as to produce a hemispherical shell. This was mounted with water on both sides of the hemisphere and with the figure-axis angle $\psi = 0$. The incident wave was a four-cycle sine wave burst of frequency 701 kHz. Figure 5 shows the resulting hydrophone output for the case of exact backscattering ($\gamma = 0°$). The earliest echo is the specular echo while the third echo (on the right-hand side of Fig. 5) exhibits focusing. Figure 6 shows the normalized hydrophone output for the third echo plotted as a function of the backscattering angle γ. This plot verifies the presence of axial focusing and shows that the width of the main lobe is similar to those shown in Fig. 2 and 4. Since the frequencies for these 3 figures were similar, we may surmise that the echoes considered were each due to the same Lamb mode.

The cause of the second echo in Fig. 5 is unclear at the time of this writing. Data indicate that this echo may also be focused.

Consideration of Fig. 3(b) shows that the mechanism for producing focused echoes can be present even if the sector of the shell is smaller (or larger) than that of a hemisphere. Hence, analysis of this problem should be helpful for understanding high-frequency scattering from elastic objects containing sectors of shells in water.

IV. Diffraction Catastrophes and Other Directional Caustics

A. Motivation and Review

Diffraction catastrophes are a class of foci which occur in various acoustical and optical problems[1,2,11,G1] They are important for describing the wavefield since purely geometrical propagation rules give unphysically divergent amplitudes at foci as the wavelength vanishes. Item C1 (reproduced here as Appendix II) discusses this divergence and reviews other aspects of catastrophes.

In previous research, we discovered that catastrophes are present in the far-field scattering of light from spheroids[11] and that the resulting diffraction pattern is useful for solving a restricted class of inverse scattering problems.[A1,G1] As noted below, the resolution of issues raised during these optical scattering experiments has advanced the understanding of acoustical diffraction catastrophes.[B1,C1]

B. Wavefronts Which Produce Transverse Cusp Diffraction Catastrophes: The Simplest Shapes

Figure 1 of Appendix II illustrates the geometry used to describe the propagation from an "exit" plane (x,y) to an observation plane (u,v). Then Eq. (II2a), where II refers to Appendix II, describes the pressure in the exit plane. The problem is to find the simplest form for the phase $g(x,y)$ for which a cusp diffraction catastrophe appears in the (u,v) plane a distance z away. The result is given by Eq. (II2b) which is

$$g(x,y) = a_1x^2 + a_2y^2x + a_3y^2, \tag{4}$$

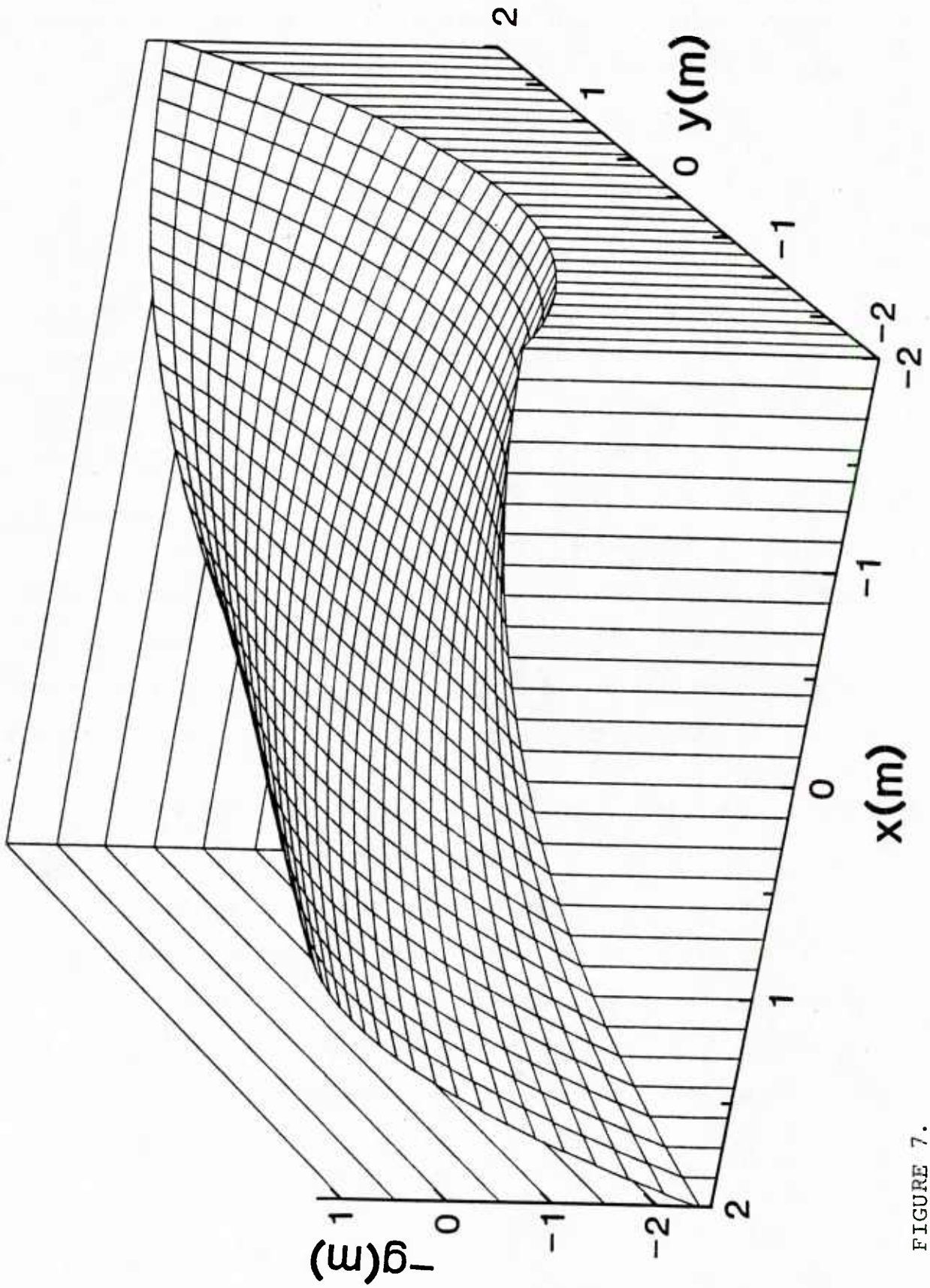

FIGURE 7.

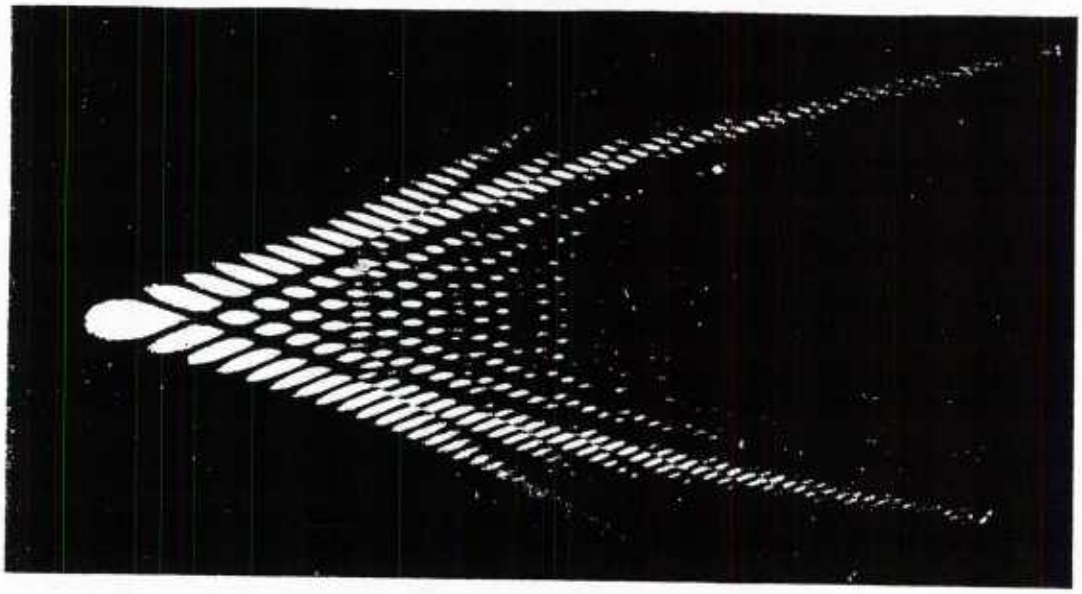

FIGURE 8(a).

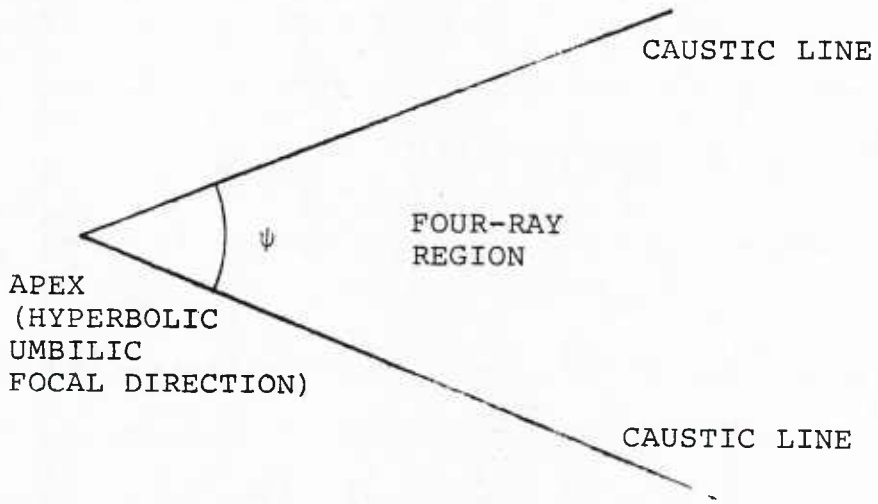

FIGURE 8(b).

where $a_2 \neq 0$ and $a_1 \neq -(2z)^{-1}$. Subsequent to the preliminary analysis of this problem in the previous Annual Summary Report,[G1] several advances were made including:[B1,C1]

(i) lifting a previous restriction that z lie in the far-field;

(ii) complete reduction of the diffraction integral to the Pearcey form;

(iii) inclusion of the optional term a_3y^2 in Eq. (4); and

(iv) analysis of the sites of rays in the exit (x,y) plane and the merging of sites for (u,v) at a caustic.

As discussed in Ref. B1, the g(x,y) may include linear terms and other small higher-order terms; however, the form of Eq. (4), with $a_3 = 0$, contains the essential features of the shape of the outgoing wavefront at (or near) the exit plane. Figure 7 shows the shape of such a representative wavefront. The parameters (chosen to simulate the reflection of underwater sound from a curved surface) were:

$$a_1 = 0.2\ m^{-1},\ a_2 = 0.2\ m^{-2},\ a_3 = 0.$$

It may be shown[B1] that -g(x,y) well approximates the shape of such a wavefront near the exit plane. Computational assistance for this, and other figures in item B1, was provided by W. P. Arnott, a graduate student supported by this contract.

C. Hyperbolic-Umbilic Diffraction Catastrophes: The Wavefront Shape

Figure 8(a) shows the hyperbolic-umbilic diffraction catastrophe which occurs in the far-field scattering of light from oblate drops of water.[11,A1] Catastrophe theory[12] indicates that (i) this pattern decorates the region near where caustic lines meet with an apex angle ψ shown in Fig. 8(b); and (ii) these caustic lines separate the observation plane into a zero-ray region and a four-ray region (according to the number of ray sites in the exit plane). To give a quantitative description of this pattern we must first specify the

associated phase (or wavefront shape) g(x,y) in the exit plane. Marston has demonstrated that g is of the form

$$g(x,y) = (\alpha x^3 + 3\gamma y^2 x)/6, \tag{5}$$

where here α and γ are parameters. The essential feature is that the term quadratic in x^2 in Eq. (4) has been replaced by a cubic term. The form of Eq. (5), though not the usual one[12] which appears in the literature on catastrophe optics (which is $g = \beta(x^3 + y^3)$) may be obtained by a smooth mapping from that form. The real test of the correctness of Eq. (5) comes by applying the Stationary Phase Condition and the Hession Condition $H = 0$ as discussed in Ref. B1 and 12. This results in the caustic lines shown in Fig. 8(b) such that the apex angle is

$$\tan(\psi/2) = (\gamma/\alpha)^{1/2}. \tag{6}$$

D. Calculation of the Parameters for Wavefronts Resulting from Reflection or Refraction by Smooth Curved Surfaces: An Example from Light Scattering and Novel Experimental Data

To calculate the apex angle ψ for the specific case of scattering from an oblate drop Fig. 8(a), the ratio γ/α is needed for the optical wavefront as it leaves the drop. See Eq. (6). To apply Eqs. (4) and (5) to problems involving the reflection or scattering of high-frequency sound (so as to describe the wavefield near the caustic) the parameter sets (a_1, a_2, a_3) and (α,β) are needed. Marston has formulated a procedure whereby these parameters may be found and has confirmed it for the case of light scattering from an oblate drop.

The procedure is summarized as follows:

(i) Locate the most singular ray (which corresponds to the one to the apex point in Fig. 8(b)).

(ii) Calculate the local principal curvatures of the wavefront associated with rays adjacent to the most singular ray found in (a). It is necessary to find these curvatures before and after each reflecting or refracting surface of the system.

(iii) The principal curvatures near the singular direction of the outgoing wavefront contain the information needed for the desired parameters.

To illustrate properly (iii), the wavefront specified by Eq. (5) has the following principal curvatures in the plane $y = 0$:

$$k_1 = \alpha x, k_2 = \gamma x \qquad (7a,b)$$

as one moves away from the planar umbilic point[12] at $x = 0$, $y = 0$. The problem then reduces to finding the coefficients of x in Eq. (7) for the outgoing wavefront. These coefficients are obtained by tracing the local principal curvatures of the wavefront as it propagates through the system from the source up to the exit plane. Kneisly[13] has presented a formalism for tracing the curvatures through a reflecting and/or refracting system. Though this formalism is said to be useful in the design of optical instruments, the present applications to scattering and acoustical problems appear to be novel.

To test the entire procedure, Marston carried out the required wavefront trace for once-reflected (twice-refracted) rays through an oblate drop. For the hyperbolic-umbilic diffraction catastrophe (h.u.d.c.) to be produced, the axis-ratio "D/H" of the oblate drop is related to the refractive index m by[14,A1,G1]

$$D/H = [3\, m^2/4\, (m^2 - 1)]^{1/2}, \qquad (8)$$

where the drop's symmetry axis is vertical and the incident light propagates horizontally. The trace was carried out for an oblate drop specified by Eq. (8) with rays in the horizontal equatorial plane because of the condition $y = 0$ on Eq. (7). The result for α and γ gives

$$\tan(\psi/2) = (\gamma/\alpha)^{1/2} = m/(12)^{1/2}. \qquad (9)$$

For drops of water in air, m = 1.332 so that Eq. (9) gives $\psi = 42.1$ deg. As noted in Ref. 11, ψ may be as large as 43.5 deg though the clearest set of data gives $\psi = 42 \pm 2$ deg in agreement with Eq. (9).

It would be desirable to verify Eq. (9) for the case of a liquid drop having another value of refractive index m. It is necessary, however, that the acoustic levitation system[11,A1] be capable of suspending the drop such that the aspect ratio D/H is given by Eq. (8). The equilibrium shape of a drop in a standing wave was calculated by Marston et al.[15] This theory was recently tested and confirmed by Trinh and Hsu[16] for D/H close to unity. For the levitation apparatus presently here at W.S.U., the candidate liquid having the largest value of m is microscope immersion oil for which m = 1.515. Indeed, the h.u.d.c. was observed and found to have an appearance similar to that of Fig. 8(a). The apex angle was measured approximately (in real time) as $\psi_{exp} \approx 46 \pm 2°$ while Eq. (9) gives $\psi_{theory} = 47.2°$. Unfortunately the pattern cannot be photographed without modifications of the apparatus.

It also appears that Kneisly's method[13] of wavefront tracing may be applied to predict and/or locate diffraction catastrophes resulting from the reflection or refraction of sound from curved surfaces.

E. Reflection of Sound Pulses from Surfaces of Negative Gaussian Curvature

Let the acoustic medium have a uniform velocity distribution. The outgoing wave front will have a local Gaussian Curvature[12,G1] $K_{w.f.}(x,y) = 0$ at those points (x,y) where the normal is directed toward a far-field caustic. An example of such a point is x = 0, y = 0 in Fig. 7. In typical reflection problems a wavefront which is nearly flat reflects from a surface for which the Gaussian Curvature $K_{surf} > 0$. The reflected wavefront diverges in such a way that $K_{w.f.} > 0$.

Reflection of a plane wave off of a surface for which $K_{surf} < 0$ will produce an outgoing wavefront for which $K_{w.f.} < 0$. Such a reflection of a transient pulse should result in a distortion of the pulse's shape in the far field.[1] It is desired to study this distortion for the reflection of ultrasonic pulses in water. The effort during the present contract period has been on the design of a suitable reflecting surface.

F. Scattering from Objects with Spherical Symmetry: A Novel Expression for the Virtual Source Location

The tracing of rays in problems related to scattering of sound from spheres (or the scattering of light from spherical drops or bubbles) is formally like that for the scattering of particles from a central potential. Typically the outgoing rays appear to diverge from a point near (or within) the scatterer which represents the location of the virtual source of the scattered waves. In the case of glory scattering it is helpful to rotate the ray diagram (Fig. 1 of Appendix I) about the symmetry axis CC' so that the virtual source at F_R traces out a ring. For the case of surface-wave glories (as in this figure) the plane which contains this ring also contains the center of the sphere.[4] In other problems the plane of the ring is displaced from the center of symmetry; the phase Φ_g of the glory wave in the far-field will depend on the backscattering angle γ via[3,17,18]

$$\Phi_g(\gamma) = - kD(1 - \cos\gamma) + \Phi_c, \qquad (10)$$

where Φ_c is a constant which may be determined geometrically. Here D is the distance of the center of symmetry from the plane of the ring. For acoustical scattering from fluid spheres[3] or the optical scattering from bubbles, the plane lies behind the center and $D > 0$.

The virtual source location may be a useful concept in other scattering problems. For example, there has been considerable recent interest[19] in modeling the glory of waves scattered by the astrophysical objects known as "black holes." A simple description of the

phase Φ_g was not given since expressions for D and Φ_g; i.e., Eq. (10), had not been obtained.[20]

For these, and other reasons (related to scattering from coated bubbles) Marston derived a general expression for D, the source distances. The method is a generalization of the one introduced by Langley (Appendix B of Ref. 21). The result is

$$D = \pm (d\theta/db)^{-1} \tag{11}$$

where $\theta(b)$ is the scattering angle for an incoming ray having an impact parameter of b (relative to the center of symmetry). The sign of Eq. (11) may be determined from geometrical rules. This result agrees with special cases discussed in Ref. 3, 7, 21, and 22. For the case of surface-wave glories, it may be argued that $|d\theta/db|$ diverges so that D vanishes as previously noted[4,6] while at rainbows $|d\theta/db| \rightarrow 0$.

V. Light Scattering from Bubbles in Water: Consideration of "Real" Versus "Ideal" Bubbles

A. Motivation and Review

This contract has previously supported research towards understanding the scattering of light from bubbles in water. The general approach and some possible applications in acoustics were reviewed in the previous Annual Summary Report.[G1] Until recently the research emphasized the case of spherical bubbles having a gas-liquid interface free of adsorbed layers of molecules.

B. Observations and Theory of Optical Backscattering from Freely Rising Bubbles in Water: The Unfolded Glory of an Oblate Bubble

During the past year the student working on this project, W. P. Arnott, has made considerable experimental, computational, and theoretical progress. It is anticipated that a

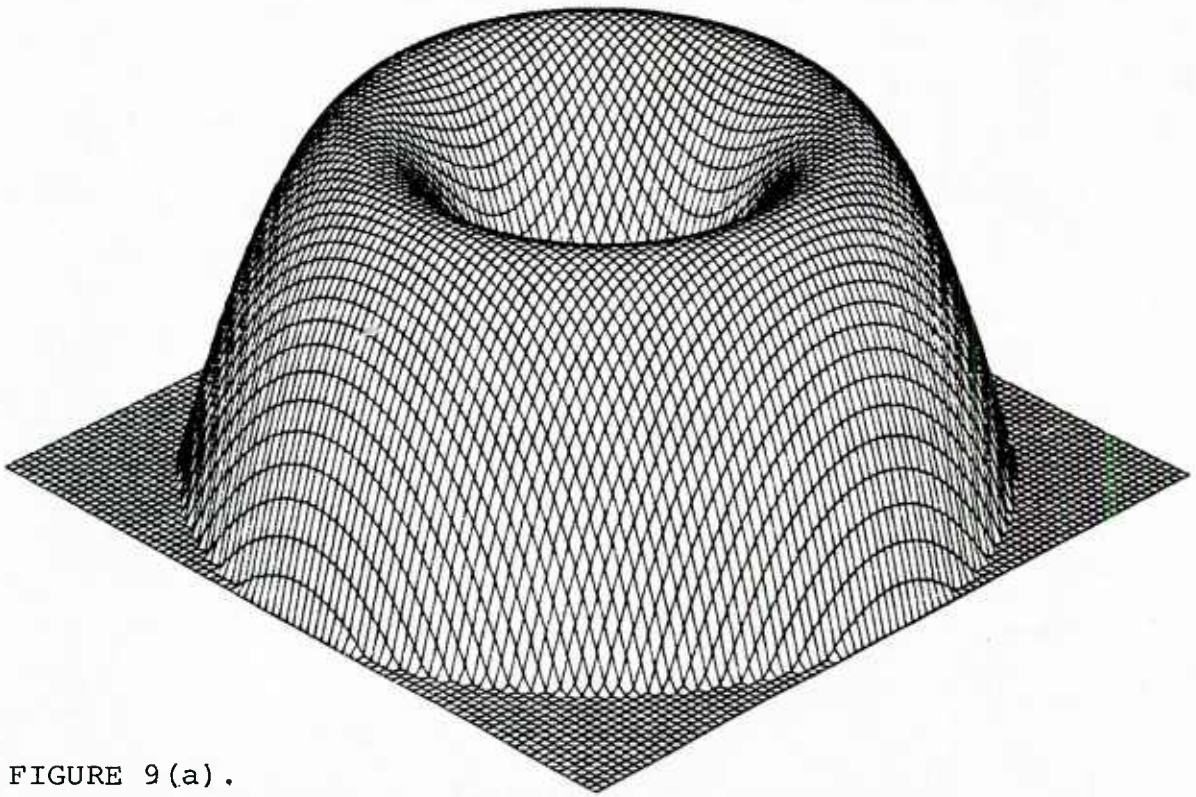

FIGURE 9(a).

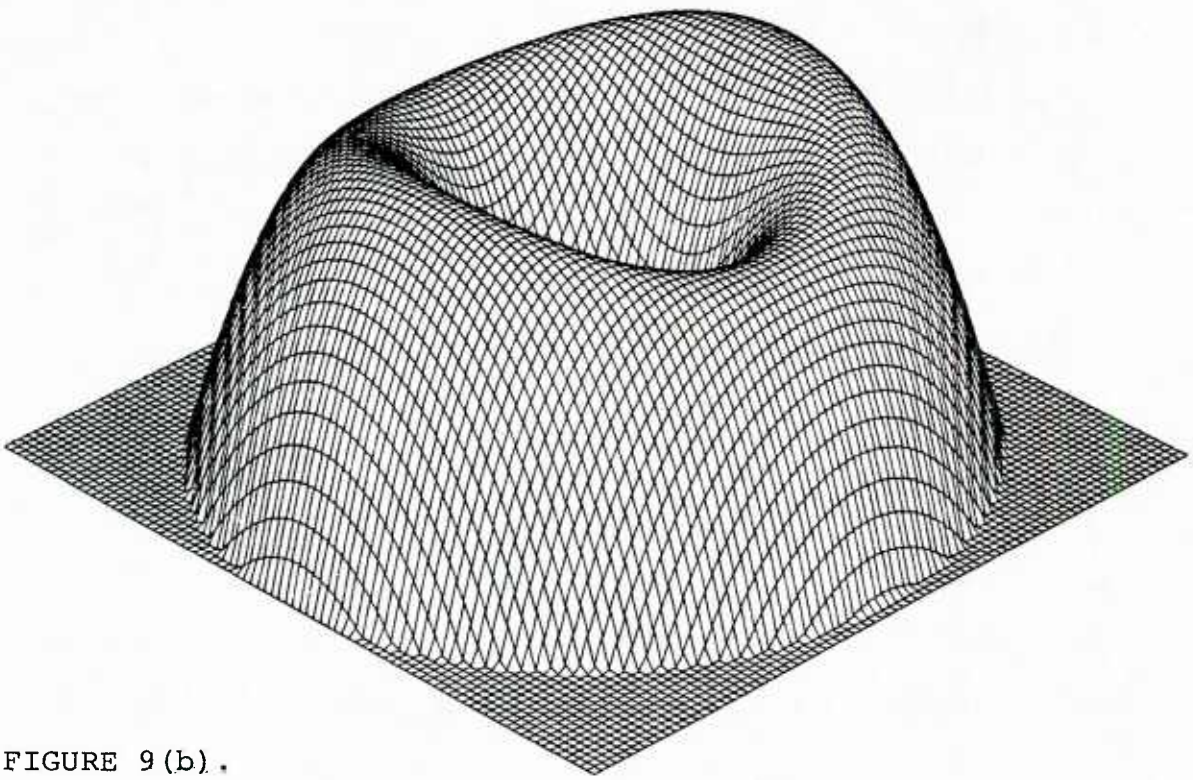

FIGURE 9(b).

manuscript describing this research will be prepared during the next year so that the present discussion will be largely qualitative (see also Ref. 23).

Freely rising bubbles in water are subjected to hydrodynamic stresses which deform the bubbles into a shape closely resembling that of an oblate spheroid[21] with a vertical axis of rotational symmetry. In these experiments, the diameter D of the bubble is typically > 0.25 mm; D is measured by collecting the bubble against a glass plate after it rises through the scattering chamber. The aspect ratio (width/height) ≡ (D/H) may then be well approximated from known hydrodynamic theory for a freely-rising bubble. Typically, $(D/H) - 1 \approx 10^{-3}$; the bubbles are nearly spherical. Nevertheless, the cross-polarized backscattering pattern can differ significantly from that of spherical bubbles in viscous oils previously photographed.[17,22]

For scattering from a spherical bubble the relevant outgoing wavefront has the local shape of a circular or parabolic torus as is illustrated in Fig. 9(a). The ray diagram for constructing this torus has been previously discussed.[3,17,22] The expanding wavefront is said to be "axially focused" along the symmetry axis of the torus. Furthermore, inspection of Fig. 9(a) shows there to be an infinite number of points for which the normal is parallel to the symmetry axis. These points lie on a circle on the wavefront where the Gaussian curvature of the wavefront $K_{w.f.} = 0$. The axial caustic is said to have an infinite co-dimension[24] because of the infinity of rays in the focal direction.

Now consider the problem of backscattering from a horizontally illuminated oblate bubble having a vertical axis of rotational symmetry. In the horizontal equatorial plane the bubble boundary is circular and the ray diagram is the same as that for spherical bubbles.[17,22] Consider now that vertical plane which contains the symmetry axis. In that plane the boundary is elliptical which results in a shifted optical path length. These shifts of the path length change the shape of the outgoing wavefront from that of Fig. 9(a) to the shape in Fig. 9(b), where the shift has been greatly exaggerated for clarity. Inspection of Fig. 9(b) shows that there is now only a finite number of points (four) where the normal is

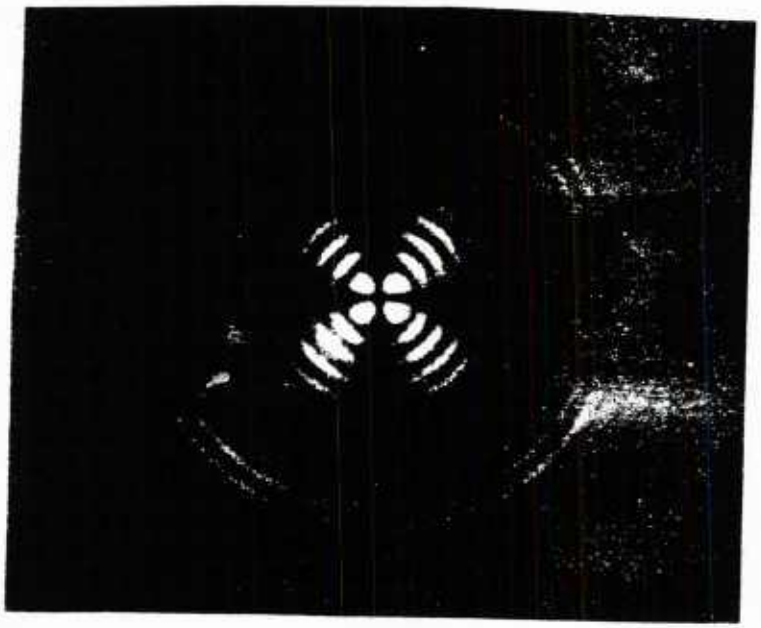

BACKSCATTERING PATTERN FOR A SPHERICAL BUBBLE IN WATER.

FIGURE 10.

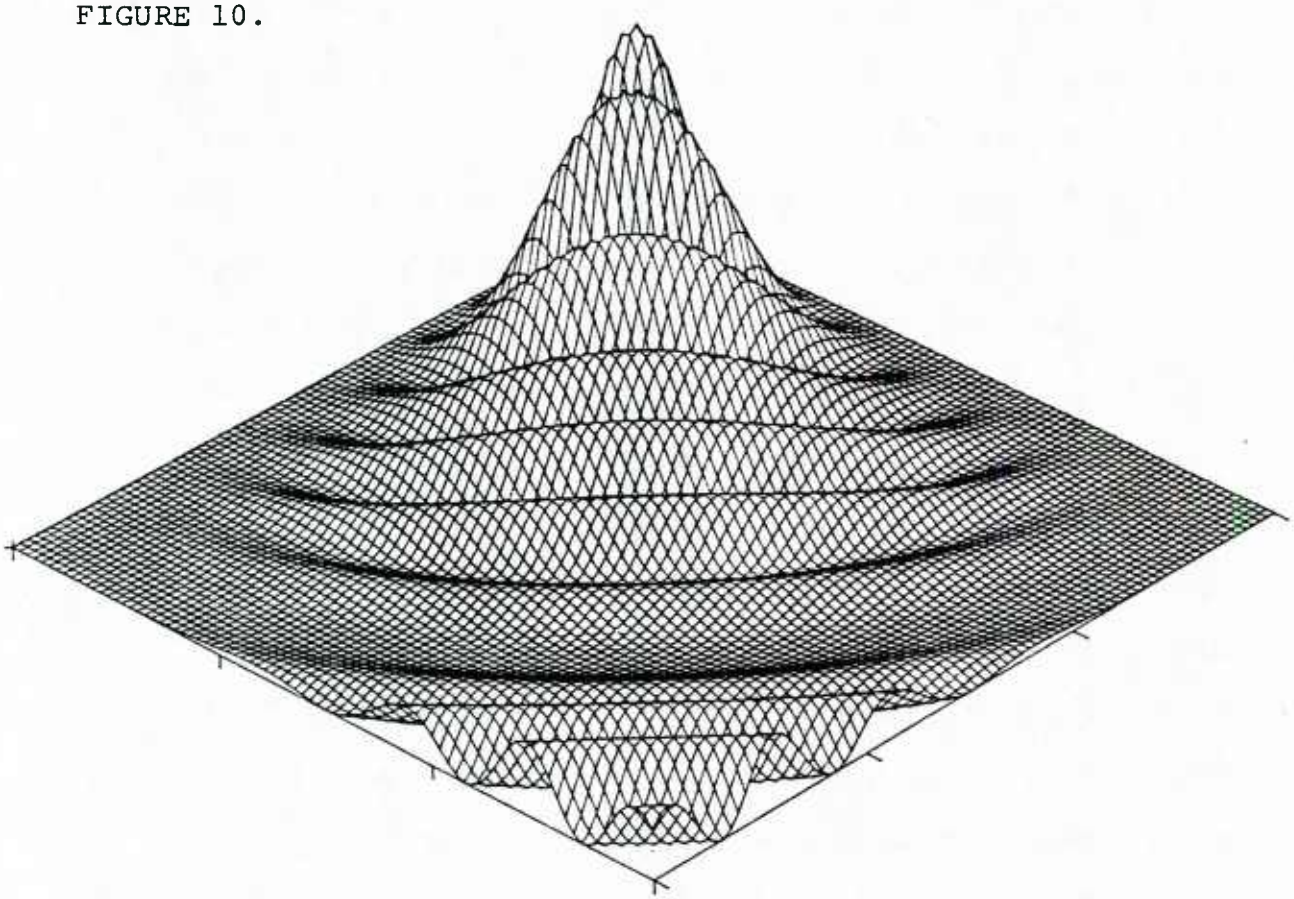

QUADRANT OF THE MODELED PATTERN FOR THE SCATTERED IRRADIANCE.

FIGURE 11.

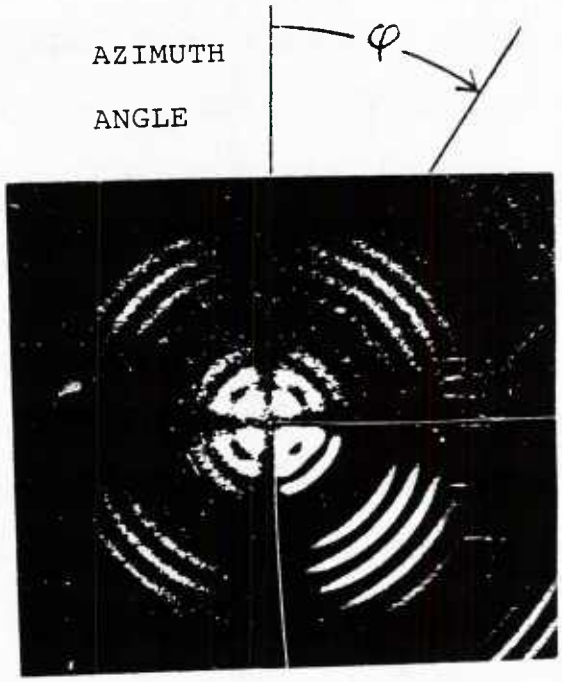

BACKSCATTERING PATTERN OF AN OBLATE BUBBLE RISING IN WATER.

FIGURE 12.

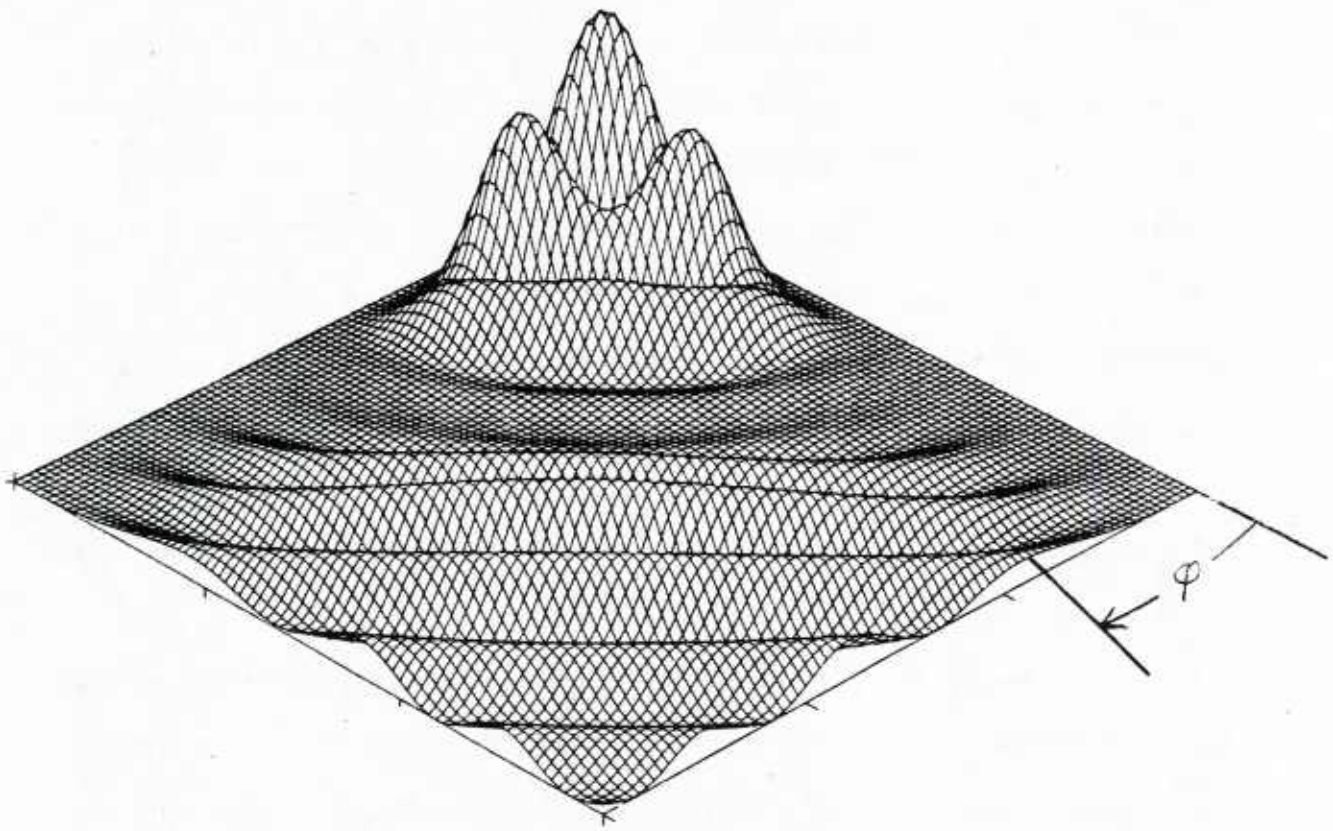

FIGURE 13. QUADRANT OF THE CALCULATED IRRADIANCE PATTERN.

parallel to the backscattering axis. The broken symmetry of the spheroid has (in the language of catastrophe theory) "unfolded" the axial caustic which would otherwise have an infinite co-dimension. The resulting scattering patterns have some fundamental significance since they illustrate the effect of such an unfolding.

The measurement configuration used by Arnott is similar to that used in our previous work on glory scattering.[17,22] The important differences are: (i) the illumination is now vertically-polarized light (from an Ar-Ion laser) having a wavelength in air $\lambda_a = 514$ nm and (ii) the bubbles rise freely in water through the scattering chamber, having been created on a needle about 10 cm below the chamber. The camera is aligned to record the cross-polarized far-field scattering into an angular region centered on the backward axis. The width of the region observed is about 9 degrees.

Figure 10 shows the scattering pattern for a freely rising bubble in water having a measured diameter $D_m = 0.255$ mm. Calculations and the previous experiments on bubbles in oil[17,22] show that the cross-polarized backscattering from a sphere should: (i) have a four-fold azimuthal symmetry about the backward axis; and (ii) the cross-polarized backscattering should vanish in the exact backward direction which corresponds to a backscattering angle γ of zero. Figure 10 is seen to be in qualitative agreement with these predictions. The angular interval $\Delta\gamma$ between the bright rings is approximately 0.19 deg. Comparison of Fig. 10 with preliminary results shown in Fig. 13 of the previous Annual Summary Report[G1] shows that Arnott has significantly reduced the amount of background optical noise. Figure 11 shows one quadrant of the modeled scattering irradiance pattern. The diameter of the bubble used in this calculation was adjusted to fit certain features of the data; the resulting diameter was $D_{calc} = 0.244$ mm.

For comparison, Figure 12 shows the scattering pattern for a larger bubble which had measured diameter $D_m = 0.334$ mm. The angular interval $\Delta\gamma$ between the bright rings is approximately 0.13 deg. One quadrant of the scattering pattern has been replaced by a synthesized scattering pattern discussed below. Inspection of the original photograph

indicates that pattern is no longer four-fold symmetric about the backward axis. Let φ denote the azimuthal angle as measured relative to the incident wave's E-field polarization axis. The observed irradiance of the second fringe from the center has a minimum near φ= 45 deg. Cross-polarized backscattering from spheres is predicted to have a $\sin^2(2\varphi)$ azimuthal dependence[17,22] which is maximized at $\varphi = 45°$ as evident in Figs. 10 and 11. The pattern in Fig. 12 shows a two-fold (or reflection) symmetry about the line $\varphi = 0$ and it manifests the aforementioned "unfolding" of the optical glory.

Figure 13 shows one quadrant of the modeled pattern of the scattered irradiance for a bubble of diameter $D_{calc} = 0.337$ mm. Here D_{calc} was selected to best reproduce the measurements shown in Fig. 12 and is in good agreement with the measured value of 0.334 mm. The oblateness for the bubble incorporated in the model was calculated from hydrodynamic theory for a freely rising bubble of diameter D_{calc}. The theory introduces the leading perturbation to the toroidal wavefront resulting from a small deviation from sphericity. (The effect of this perturbation on the shape of the wavefront is seen by comparing Fig. 9(b) with 9(a).) Figure 13 and the synthetic quadrant of Fig. 12 show that this perturbation technique satisfactorily describes measured patterns. The synthetic quadrant in Fig. 12 makes the comparison between experiment and theory easier because the two patterns have the same angular scales.

The agreement between model and experiment shown here is representative of other case studies for which $D < 0.4$ mm. Large bubbles, say $D > 0.6$ mm, exhibit a qualitatively different backscattering pattern for which our perturbation approach may not be applicable.

The brightness of the patterns seen in Fig. 10 and 12, relative to that of the background, support the suggestion[1] that it may be possible to detect sound by illuminating bubbly water with a laser so as to monitor the modulation of the backscattered light.

Wavefront perturbations, similar to that illustrated in Fig. 8(b), will also occur in the unfolding of acoustical axial caustics discussed in Sec. III. The analysis will be similar to that of the optical scattering problem discussed here.

C. Scattering of Light from a Coated Spherical Air Bubble in Water: A Computational Study of the Optical Effects of Adsorbed Films

There is considerable evidence that bubbles in the ocean become coated by adsorbed molecules which inhibit the diffusion of gas to (and from) the bubble. One consequence of the reduction of the diffusion rate is that coated bubbles may take a long time to dissolve.[25] The acoustical resonance properties of bubbles may be affected by a film of adsorbed molecules; however, there are no published data which clearly support such a claim. With the partial support of this contract, a graduate student Stuart C. Billette developed and tested computer programs for calculating the light scattering from a spherical bubble in water coated by a film of uniform thickness. The method used was to evaluate the electromagnetic partial-wave series given by Aden and Kerker[26] for the general concentric sphere problem. The bubbles of interest were typically very much larger than the optical wavelength so that the computation of this series is nontrivial. Billette's M.S. thesis discusses the computer programs and gives numerous curves for the calculated irradiance as a function of scattering angle. This thesis[H1] is to be issued to DTIC as a Technical Report so that the summary given here will be brief.

During the course of this investigation the research support for Billette and Marston was partially transferred to a contract with related goals.[27] This was done to facilitate research on specific topics relevant to the development of an optical bubble-size spectrometer by Dr. Ming-Yang Su (Oceanographer, Naval Ocean Research and Development Activity).

Figure 14 is an example of a computational result relevant to the design of a bubble size spectrometer. Let a denote the radius of a spherical air pocket and let h denote the thickness of the coating which surrounds it. The water (which is outside of the coating) is

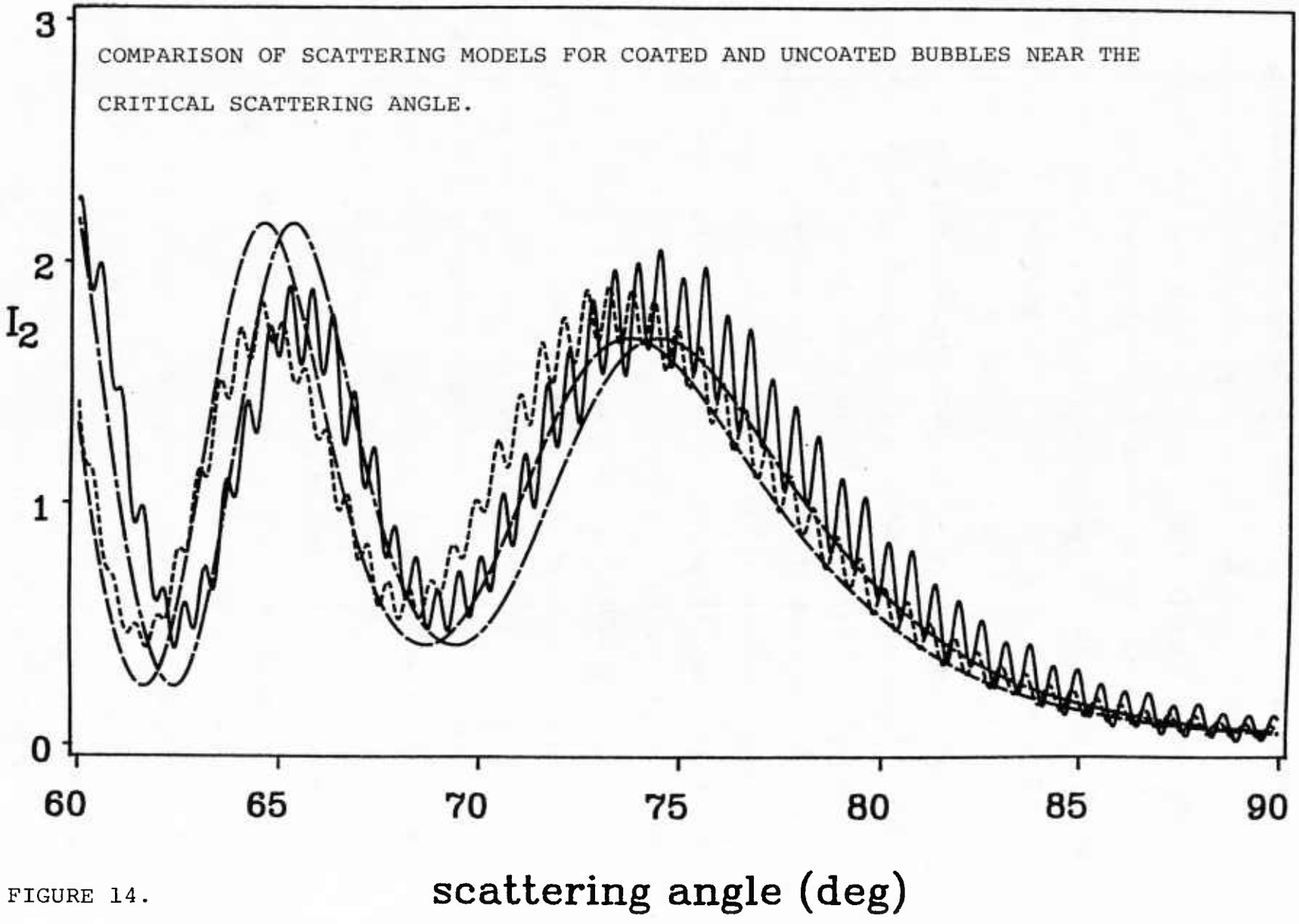
COMPARISON OF SCATTERING MODELS FOR COATED AND UNCOATED BUBBLES NEAR THE
CRITICAL SCATTERING ANGLE.
3
2
1
0
I_2
60
65
70
75
80
85
90
scattering angle (deg)

FIGURE 14.

taken to have a refractive index of $4/3 \approx 1.333$ while the refractive index of the coating is 1.5. Figure 14 shows the scattered irradiance for polarized light for the case in which the E field is parallel to (i.e., lies within) the plane of scattering. In all of the curves $a = 37.8$ μm. The solid curve is for a coated bubble with $h = 1$ μm and was given by the exact partial-wave series. The curve with short dashes is for an uncoated bubble and was given by the Mie series. These numerical values for h and a are for the case of red light having a wavelength in air of 633 nm. The slowly varying curve with short dashes is the result of the previous physical-optics approximation (POA) for scattering from a homogeneous bubble previously formulated by Marston and Kingsbury (see, e.g., Ref. 21). That curve is seen to approximate the coarse structure in the Mie curve (as well as the data for scattering from uncoated bubbles, see Ref. 21). The right-most smooth curve (which alternates along with a short dash) is a shifted plot of the POA curve. That shift was calculated geometrically by Marston so as to obtain an approximate description of the scattering from a coated bubble near the critical scattering angle ≈ 82.8 deg.

Figure 14 shows that the principal effect of the coating on the coarse structure is to shift slightly its angular location and its quasi-period. Notice, however, the coarse structure should not be masked by the presence of the coating. Hence size spectrometers which make use of the coarse structure should still function if the bubble is coated. The coating may, however, introduce a small error (or shift) in the bubble size estimated from scattering data. It is noteworthy that the effects of the coating on the orthogonal polarization (E-field perpendicular to the scattering lane) were much more significant; that choice of polarization may be unsuitable for use in a size spectrometer. These polarization effects may be explained in terms of physical arguments.[H1]

These calculations also suggest that the polarized irradiance scattered near the Brewster scattering angle of 106 deg may, if suitably averaged over angle, be a monotone increasing function of the film thickness h. Hence measurements of this averaged Brewster angle irradiance may be useful for estimating the film thickness on freely rising

bubbles in sea water.[H1] The fine structure near this angle may also be useful for determining h.

VI. Production of Sound by a Pre-existent Bubble in Water Illuminated by Modulated Light: A Novel Photo-Acoustic Source and Related Experiments on the Sounds Produced by Illuminated Drops

A. Review and Summary

The previous Annual Summary Report[G1] describes experiments and a simple model for the production of sound by bubbles in water illuminated by modulated laser light. These experiments[F1] and the development of an appropriate theory are the Ph.D. dissertation problem of a graduate student B. T. Unger. Unger has written a draft of his dissertation (which is now being revised). He is presently teaching high school science so as to qualify for certification as a teacher. Unger is not presently supported by this contract; however, it is anticipated that the dissertation will be completed and available in report form prior to May 1987. Consequently the present report will only outline the past year's progress.

The experimental work was limited by equipment problems, primarily because the digital signal averager had to be returned to the manufacturer because the power supply failed (which evidently damaged other components). Nevertheless there were several noteworthy accomplishments:

(1) The sound radiated by a bubble in response to an optical burst of four pulses was detected using the procedure previously discussed.[G1] In these new experiments the fundamental frequency f of the burst was initially set at the frequency f_O of the bubble's monopole resonance. It was subsequently set about 15% above (and then below) f_O. The sound radiated for the cases $f \neq f_O$ was lower in amplitude than for the case $f \approx f_O$ as is to be expected from the previously outlined model.[G1]

(2) The sound radiated by a bubble illuminated by four pulses having $f \approx f_O$ was detected as previously discussed. Recall[G1] that the incident laser beam used in these experiments corresponds to the TEM01* or "doughnut mode"; there is an irradiance minimum at the center. In the experiments, the peak optical power, determined by the laser and modulator system, was held constant at a value close to 1 watt. The relative magnitude of the sound radiated was measured for different bubbles for several values of the optical beam width. Though the measurements are somewhat qualitative the amplitude depends on the ratio of the bubble radius to beam width. See item (4) below.

(3) The impulse response of the acoustical detection system was studied for various thermal acoustic sources including dyed drops of oil illuminated by modulated laser light and small pulsed electrical heating elements (i.e., resistors). This study was useful for calibration purposes.

Theoretical advances included:

(4) An improved model was developed for the radial projection of the optical radiation stress on the bubble. This stress is thought to be the principal mechanism whereby the bubble is set into vibration so as to radiate sound.[G1] The model predicts that the stress will be a sensitive function of the ratio of the bubble radius to the beam width. As noted in item (2) above, the magnitude of the radiated sound was seen to depend on this ratio.

(5) Improved models were developed for the radiation of sound from thermal-acoustic point-like sources. Such sources include the case of a small dyed oil drop illuminated by modulated light and (as a rough approximation) the case of a pulsed heater in water. The models are relevant to the calibration experiments noted in item (3) above.

VII. Acoustical Phase Conjugation

A. Introduction and Review

The principal objectives of the proposed research[1] is to examine physical mechanisms for producing acoustical phase conjugating mirrors (PCM) and to verify certain focal properties of the conjugate wave. It will be assumed that the reader is cognizant with the early Soviet research on acoustical phase conjugation[28] and with the analogy of a PCM with a real-time hologram which acts so as to focus the conjugate wave toward the source. The research during the present contract period has been concerned either with understanding novel mechanisms or with basic theory.

B. The Focal Location of the Conjugate Wave Depends on a Ratio of Frequencies (A Novel Result)

Soviet experiments (Kustov et al.[29]) carried out where the frequency f_3 of the "conjugate" wave was different from the frequency f_2 of the "signal" wave. In those experiments the PCM consisted of a layer of bubbles rising in water which were insonified by a large amplitude pump wave having a frequency $f_1 = 100$ kHz. The signal incident on the PCM was radiated from a point-like source having $f_2 = 60$ kHz. The nonlinear response gave rise to a "conjugate" wave having a frequency $f_3 = f_1 - f_2 = 40$ kHz. Measurements of the width of the conjugate beam, as a function of the distance z from the bubble layer, were presented as evidence of focusing towards the source. Presumably the researchers did not examine true phase conjugation, which would require that $f_2 = f_3 = f_1/2$, because of problems with spurious signals.

Marston has shown theoretically that the focal location of the "conjugate" wave will be displaced from the source when the frequency $f_3 \neq f_2$ as in that experiment. Let z_2 and z_3 denote the distance from the plane of bubbles to, respectively, the point-like source and the focus of the conjugate wave. Marston's analysis, which is based on a relationship

between the phases of the signal and conjugate waves at the bubble layer yields the condition:

$$z_3 \approx z_2 (f_3/f_2) \tag{12}$$

for paraxial rays. This result can also be inferred from the well known change of scale for an optical holographic image which occurs when the image is "played back" at a different wavelength from that used during the recording of the original hologram. Indeed, Eq. (12) corresponds to a special case of an equation governing the image location in the holographic problem.[30]

The focal shift implied by Eq. (12) was not mentioned in Ref. 29 though it does not appear to be inconsistent with the data presented.

C. Novel Phase Conjugating Mirror for Use in Water

To study the detailed focal and temporal properties of an acoustical phase conjugated wave, it would be desirable to replace the bubble layer used by Kustov et al.[29] by a stable layer of bubbles. Marston has considered various ways of doing this. The following method is suggested: Nuclepore[31] filters consist of a membrane with uniformly distributed pores running through the membrane. The pore size is sharply defined by the manufacturing process. With suitable treatment the pores will contain a stable gas-filled cavity or microbubble. Furthermore these cavities exhibit a significant nonlinear response to ultrasound.[32] Because the number density of pores may be quite large ($> 10^5$ pores/cm^2) it would seem that the associated trapped microbubbles should exhibit the nonlinear response required to mix the signal wave (frequency f_2) with the pump wave (frequency f_1) so as to produce the conjugate wave at frequency $f_3 = f_1 - f_2$.

Nuclepore membranes are flexible. Therefore it should be possible to study how the shape of the bubble layer affects the focal properties of the conjugate wave.

D. Phase Conjugation Due to the Reflection of Sound from a Vibrating Surface

Consider the reflection of sound incident with a frequency f_2 from a surface which vibrates at a frequency f_1. It is well known that the spectrum of the reflected wave is Doppler shifted so as to include the frequencies $f_2 \pm f_1$. For example, these sidebands were recently used by Cox and Rogers[32] in the case $f_1 << f_2$ to measure the amplitude of low frequency surface oscillations. Those experiments stimulated Marston to consider the special case $f_1 = 2f_2$ as a possible method of producing a phase conjugated wave. Evidently there should be a sideband produced having a frequency $f_3 = f_2 - f_1 = - f_2$. It may be argued that such a wave will be a conjugate of the incident wave and will be focused back towards the source. It turns out that the problem had already been studied in the Soviet literature though the published experimental data on the conjugate wave is somewhat unclear. Unfortunately the conversion efficiency for the production of a conjugate wave may be small unless the surface displacements are not negligible in amplitude in comparison to the wavelength.[34,35]

VIII. Other Research

Previous research, supported partially by O.N.R. Physics Division, was published. This includes experiments demonstrating rapid cavitation in water (and in ethylene glycol) resulting from the reflection of a shock pulse from a liquid surface.[C3] These experiments were novel in that the pulse duration was short (2 μsec) and that the surface velocity was measured.

Previous theoretical research had tested the physical-optics approximation for the case of light scattered from spherical bubbles in liquid helium. This research was edited and put into its final form for publication.[D1]

IX. References

1. P. L. Marston, "Propagation and Effects of Acoustical and Optical Waves" (relevant research proposal for the current contract), submitted to O.N.R. Physics Division (Oct. 1, 1985).
2. P. L. Marston, Research proposal submitted to O.N.R. Physics Division (Oct. 1, 1984) for funding period Jan. 1, 1985 - Dec. 31, 1985.
3. P. L. Marston and D. S. Langley, "Glory- and Rainbow-Enhanced Acoustic Backscattering from Fluid Spheres: Models for Diffracted Axial Focusing," J. Acoust. Soc. Am. 73, 1464-1475 (1983); 78, 1128 (1985).
4. K. L. Williams and P. L. Marston, "Axially Focused (Glory) Scattering due to Surface Waves Generated on Spheres: Model and Experimental Confirmation using Tungsten Carbide Spheres," J. Acoust. Soc. 78, 722-728 (1985).
5. K. L. Williams, Technical Report No. 5: Acoustical Scattering from an Elastic Sphere in Water: Surface Wave Glory, Resonances, and the Sommerfeld-Watson Transformation for Amplitudes, Accession Number AD-A158884 (Defense Technical Information Center, Alexandria, VA, issued August 1985).
6. K. L. Williams and P. L. Marston, "Backscattering from an elastic sphere: Sommerfeld-Watson transformation and experimental confirmation," J. Acoust. Soc. of Am. 78, 1093-1102 (1985); 79, 2091 (1986).
7. H. M. Nussenzveig and W. J. Wiscombe, "Forward optical glory," Opt. Lett. 5, 455-457 (1980).
8. P. L. Marston and D. S. Langley, "Forward optical glory from bubbles (and clouds of bubbles) in liquids and other novel directional caustics" in Multiple Scattering of Waves in Random Media and Random Rough Surfaces (edited by V. V. and V. K. Varadan) at press.
9. M. Born and E. Wolf, Principles of Optics 4th ed. (Pergamon, Oxford, 1970) Sec. 8.2.

10. C. F. Ying et al., "Study in the reflection of the Lamb wave from the plate free end face by the photoelastic visualization technique," in Proceedings of the 12th International Congress on Acoustics (Beauregard Press, Toronto Canada, 1986), pp. I3-6.1, 6.2.

11. P. L. Marston and E. H. Trinh, "Hyperbolic umbilic diffraction catastrophe and rainbow scattering from spheroidal drops," Nature (London) 312, 529-531 (1984).

12. M. V. Berry and C. Upstill, "Catastrophe Optics: Morphologies of Caustics and Their Diffraction Patterns," in Progress in Optics Vol. 18, ed. E. Wolf (North-Holland, Amsterdam, 1980) pp. 257-346.

13. J. A. Kneisly II, "Local curvature of wavefronts in an optical system," J. Opt. Soc. Am. 54, 229-235 (1964).

14. J. F. Nye, "Rainbow scattering from spheroidal drops: an explanation of hyperbolic-umbilic foci," Nature (London) 312, 531-532 (1984).

15. P. L. Marston, et al., "Quadrupole Projection of the Radiation Pressure on a Compressible Sphere," J. Acoust. Soc. Am. 69, 1499-1501 (1981).

16. E. H. Trinh and C.-J. Hsu, "Equilibrium shapes of acoustically levitated drops," J. Acoust. Soc. Am. 79, 1335-8 (1986).

17. P. L. Marston and D. S. Langley, "Strong Backscattering and Cross-Polarization from Bubbles and Glass Spheres in Water," in Ocean Optics VII, Proceedings of the Society of Photo-Optical Instrumentation Engineers 489, 130-141 (1984).

18. In the notation of Ref. 3 and 17, $D = \alpha - a$ where a is the radius of a spherical bubble and α is the distance from the exit plane to the plane of the focal circle.

19. R. A. Matzner, et al., "Glory scattering by black holes," Phys. Rev. D 31, 1869-1878 (1985).

20. Conversation with Professor R. A. Matzner, Dept. of Physics, University of Texas, Austin, April 1985.

21. D. S. Langley and P. L. Marston, "Critical-Angle Scattering of Laser Light from Bubbles in Water: Measurements, Models, and Applications to Sizing of Bubbles," Applied Optics 23, 1044-1054 (1984).

22. D. S. Langley and P. L. Marston, "Glory in the Optical Backscattering from Air Bubbles," Physical Review Letters 47, 913-916 (1981).

23. Informal progress letter (Contract N00014-85-C-0141) to L. Hargrove, O.N.R. Physics Division, April 17, 1986.

24. M. V. Berry, "Waves and Thom's theorem," Advances in Physics 25, 1-26 (1976).

25. V. V. Goncharov et al., "Determination of the diffusion constant of a gas bubble in sea water from the solution of air bubbles in the medium," Soviet Physics Acoustics 30, 273-275 (1984).

26. A. L. Aden and M. Kerker, "Scattering of electromagnetic waves from two concentric spheres," J. Appl. Phys. 22, 1242-1246 (1951).

27. O.N.R./N.O.R.D.A. Contract N00014-86-K-0242 (86 Feb 01 - 86 Sept 30) for $9999.00 for work described in the proposal "Practical Computations of the Scattering of Light from Bubbles in Water."

28. B. Y. Zeldovich et al., Principles of Phase Conjugation (Springer, Berlin, 1985) pp. 203-205.

29. L. M. Kustov et al., "Phase conjugation of an acoustic wave at a bubble layer," Sov. Phys. Acoust. 31, 517-518 (1985).

30. J. W. Goodman, Introduction to Fourier Optics (McGraw Hill, N.Y., 1968) Sec. 8-4, Eq. (8-41).

31. Nuclepore Corporation, 7035 Commerce Circle, Pleasanton, CA 94566-3294.

32. D. L. Miller and E. A. Neppiras, "On the oscillation mode of gas-filled micropores," J. Acoust. Soc. Am. 77, 946-953 (1985).

33. M. Cox and P. H. Rogers, "Acoustic response of the swimbladder in goldfish," in Proceedings of the 12th International Congress on Acoustics (Beauregard Press, Toronto Canada, 1986), pp. B6-7.1, 7.2.

34. A. P. Brysev. et al., "Plane parametric phase-conjugation mirror," Sov. Tech. Phys. Lett. 8, 241-243 (1982).

35. A. M. Kovalev and V. N. Krasilnikov, "Reflection of electromagnetic waves from moving surfaces," Sov. Phys. Tech. Phys. 7, 19-21 (1962).

SCATTERING FROM AN ALUMINUM SPHERE: FABRY-PEROT ANALYSIS OF RESONANCES BASED ON THE WATSON TRANSFORMATION

K. L. Williams[a] and P. L. Marston

Department of Physics, Washington State University, Pullman, Washington, USA 99164-2814

The partial-wave series (PWS) given by Faran [1] is useful for computing the scattering of a plane acoustic wave in water from an elastic sphere for the usual case in which viscous effects are negligible. We have recently [2] carried out a Sommerfeld-Watson Transformation (SWT) of Faran's PWS. This transformation is useful at high-frequencies where it converts the PWS to a more rapidly convergent form and allows one to ascertain the physical origin of various contributions to the scattering. In particular one can isolate the contributions from specular reflection, transmitted bulk waves, and surface waves and predict glory scattering [3].

In Sec. I of this paper we first recap some of the SWT results of [2]. We give quantitative expressions for the contributions due to the specular reflection, and Rayleigh and whispering gallery surface waves. After a brief discussion, the results for each surface wave type are recast in a novel closed form reminiscent of that used in the analysis of Fabry-Perot resonators [4,5]. The SWT analysis is confirmed by synthesizing |f|, the magnitude of the backscattering form function, for an aluminum sphere in water and comparing this synthesis with the PWS result. In Sec. II, some aspects of the present analysis are compared with aspects of Resonance Scattering Theory (RST) [6,7] and the Singularity Expansion Method (SEM) [8].

I. SWT RESULTS, THEIR INTERPRETATION, AND THE SYNTHESIS OF f.

The PWS for the scattered pressure in the far field of the sphere is commonly written [2,5,7] in terms of a complex form function f which depends both on the ka of the sphere (a is the sphere's radius and $2\pi/k$ is the wavelength in water) and the scattering angle. A harmonic time dependence of $\exp(-i\omega t)$ is assumed in our analysis. The SWT [2] facilitates approximating f as $f \approx f_S + f_{tw} + f_{sw}$ for near backscattering where: f_S is the specular reflection contribution, f_{tw} is the transmitted bulk wave contribution, and f_{sw} is the surface wave contribution and is the sum of contributions f_F, f_R, f_{WG} from Franz, Rayleigh, and whispering gallery waves respectively. Depending on ka and/or material parameters, there may be several significant Franz and whispering gallery waves though for the ka range considered here f_F should be negligible and will not be considered. The specular reflection contribution f_S has the form, Eq. 20 of [2], $f_S(x) = -R_S(x)\exp(-i2x)$ near backscattering; here $x \equiv ka$, $(-R_S)$ is the effective coefficient of reflection from the sphere given in [2], and $(-2x)$ is the phase of the specular reflection relative to a ray traveling in the liquid to and from a reference point corresponding to the sphere's center.

The contributions from the Rayleigh and individual whispering gallery waves are found from a residue analysis of complex poles ν_l and have the form (Eq. (31) of [2])

$$f_l = -G_l J_0(kb_l\gamma)\, e^{i\eta_l - 2(\pi-\theta_l)\beta_l} \sum_{m=0}^{\infty} e^{i2\pi m(\alpha_l+\frac{1}{2}) - i\pi m - 2\pi m\beta_l}$$

where l equals R for the Rayleigh wave or WG_j for the jth whispering gallery wave (by convention j = 1 corresponds to the slowest whispering gallery wave), J_0 is the zeroth order Bessel function, γ is the backscattering angle, and we have used the substitutions $\alpha_l = \mathrm{Re}(\nu_l)$ and $\beta_l = \mathrm{Im}(\nu_l) > 0$. The quantities $\theta_l, \eta_l, \beta_l, b_l, \alpha_l, G_l$ are all functions of x. The variables and summation in f_l have the following physical significance [2]: G_l accounts for the coupling efficiency of the lth wave onto the sphere as well as part of the effects of axial focusing; $J_0(kb_l\gamma)$ gives the angular dependence of the near backscattering and is characteristic of glory scattering tested experimentally in [3]; b_l is shown in Fig. 1 for the case l = R; θ_l is the local angle of incidence of the lth surface wave (see Fig. 1); and the sum over m accounts for the surface wave circumnavigating the sphere an infinite number of times. The terms $\exp(i\eta_l)$ and $\exp(-2(\pi-\theta_l)\beta_l)$ are respectively the phase delay and attenuation for the first time the surface wave radiates sound in the backward direction after having traveled from the point B to B' in Fig. 1. The terms $\exp[i2\pi m(\alpha_l + 1/2)]$ and $\exp[-2\pi m\beta_l]$ are the additional propagation phase delay and attenuation of the surface wave after m circumnavigations of the sphere and $\exp(-im\pi)$ accounts for phase shifts due to caustics at K and C' in Fig. 1.

An alternate expression for f_l can be found by use of a geometric series which appears in the analysis of Fabry-Perot resonators [4,5] from which one finds

$$f_l = \frac{-G_l J_0(kb_l\gamma)\exp[-2(\pi-\theta_l)\beta_l + i\eta_l]}{\{1+\exp[-2\pi\beta_l + i2\pi(\alpha_l+\frac{1}{2})]\}} \qquad (1)$$

This novel closed form result for surface wave contributions is convenient for steady state computations. By inspection of Eq. (1) one sees that if x is such that α_l equals an integer n the magnitude of the denominator is close to a minimum since β_l is a usually small and slowly varying function of x. Therefore, one sees a resonance behavior in $|f_l|$. In [5] this behavior was examined for the case of a tungsten-carbide sphere in water.

The above results can be used to obtain curves of |f|, the magnitude of the backscattering form function, as a function of ka for an aluminum sphere in water. In performing the analysis one uses f_S and f_l evaluated at $\gamma = 0$. The material parameters used for aluminum are a density $\rho = 2.7$ gm/cm^3 and longitudinal and transverse wave speeds of 6.420 and 3.040 km/s respectively while for water $\rho = 1.0$ gm/cm^3 and the wave speed is 1.493 km/s. In Fig. 2 the SWT result using only the specular reflection and Rayleigh contributions to |f|, given by $|f_S + f_R| \equiv f_{SR}$, is compared with the exact result using the PWS labeled f_b. The ka range was chosen to correspond to the region where |f| for the aluminum sphere has major contributions from the Rayleigh and slowest whispering gallery wave. One sees in Fig. 2 that f_{SR} is a good approximation to f_b for the lower part of the ka region shown. In Fig. 3 the contribution from f_{WG1} is included and $f_{SRWG} \equiv |f_S + f_R + f_{WG1}|$ is compared with f_b. The increased agreement is evident. This synthesis of f_b by addition of each surface wave contribution to the specular reflection allows one to see the significance of each surface wave in producing the resonance related structures.

II. DISCUSSION

The SWT is an alternate and complementary analysis of situations previously examined by RST. The SWT can be used to understand further how certain phase shifts [5] affect the structure of |f|. The reformulation of the series for f_l into the closed form of Eq. (1) is similar, in principle, to the "hybrid synthesis" technique used in SEM. The resonance condition ($\alpha_l = n$) found in Eq. (1) is close to the resonance prescriptions [5] of both RST and SEM. When |f| is synthesized using RST there is a separate term for each resonance of the lth surface wave (i.e. for each value of n) while Eq. (1) accounts for all the resonances of the lth surface wave. The physical picture (Fig. 1) ensuing from the SWT is not restricted to spheres and may be used to predict the possibility of axial focusing for objects of revolution ensonified along the symmetry axis [3].

This research was supported by the U.S. Office of Naval Research.

(a) Present address: Naval Coastal systems Center, Code 4120, Panama City, FL 32407.

[1] J. J. Faran, J. Acoust. Soc. Am. 23, 405 (1951).
[2] K. L. Williams and P. L. Marston, ibid 78, 1093 (1985); erratum (at press).
[3] K. L. Williams and P. L. Marston, ibid 78, 722 (1985).
[4] E. Hecht and A. Zajac, Optics (Addison-Wesley, MA, 1974) p. 305.
[5] K. L. Williams and P. L. Marston, J. Acoust. Soc. Am. (to be published).
[6] L. Flax, G. L. Gaunard, and H. Überall, in Physical Acoustics Vol. 15 (Academic, New York, 1981) pp. 191-294.
[7] G. L. Gaunaurd and H. Überall, J. Acoust. Soc. Am. 73, 1 (1983).
[8] L. B. Felsen, IEEE Trans. Antennas Propag. AP-32, 775 (1984).

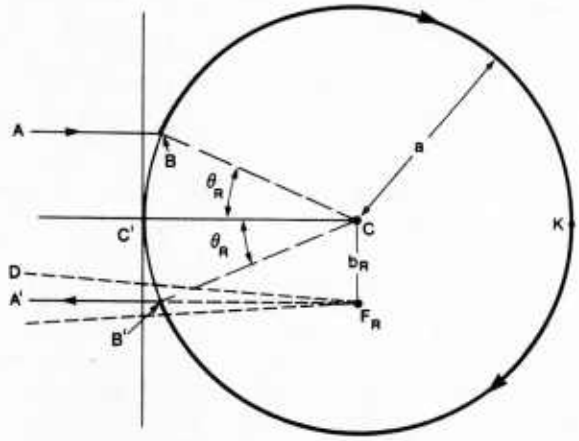

Fig. 1. Ray diagram for surface waves on a sphere.

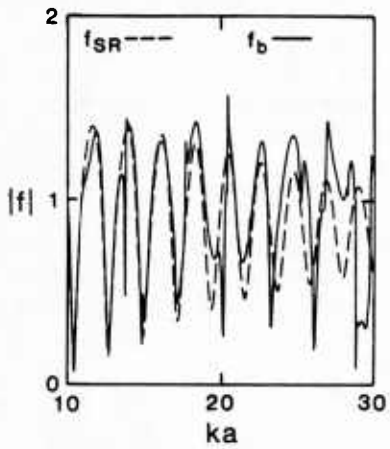

Fig. 2. |f| from PWS (solid curve) and synthesis (dashed) from Rayleigh and specular contributions.

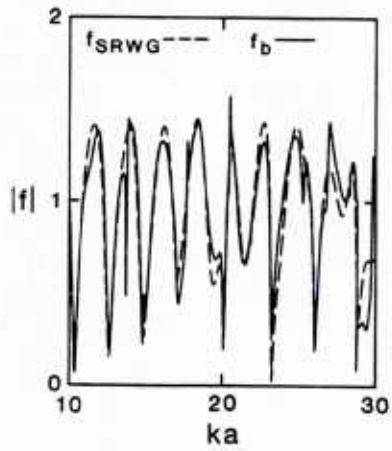

Fig. 3. As in Fig. 2 but including a whispering gallery contribution in the synthesis.

DIRECTIONAL CAUSTICS IN ACOUSTICS AND IN LIGHT SCATTERED FROM BUBBLES

P. L. Marston

Department of Physics, Washington State University, Pullman, WA 99164 U.S.A.

Caustics were investigated for acoustical or analogous optical scattering problems. Examples include the glory of elastic spheres and the optical cusp diffraction catastrophes of penetrable spheroids. The diffraction integral for the directional cusp reduces to the usual Pearcey function (known to be descriptive of a longitudinal cusp) only after a nontrivial transformation which facilitates a simple description of the outgoing wavefront. The analysis (given here) shows that the transverse cusp is not confined to the far field. Observations of novel directional caustics in the optical scattering patterns of bubbles in water (which are of interest in cavitation and ocean acoustics research) are also reviewed. Caustics appear to be particularly useful in certain inverse problems.

INTRODUCTION

To understand short-wavelength scattering and propagation problems it is important to distinguish between wavefronts which produce caustics and those which do not. Caustics at infinity (i.e. far-field foci) are produced in homogeneous media in directions where the Gaussian curvature K vanishes for an outgoing wavefront [1]. Canonical diffraction integrals can be used to show that the pressure amplitude at caustics varies as

$$p \propto (d/r)(d/\lambda)^{\beta}, \quad (1)$$

if the dependence of the attenuation on the wavelength λ may be neglected. Here r refers to the distance from the scatterer or, more generally, an exit plane where the outgoing wavefront is specified; d has the dimensions of length and is determined by the outgoing wavefront. In scattering problems d is proportional to the size of the scatterer. The Arnold singularity index β typically has values in the range $1/6 \le \beta < 1/2$ (the case [1,2] of "diffraction catastrophes") though special caustics are possible for which $1/2 \le \beta \le 1$ (see Sec. II and III). Wavefronts which are not focused are describable by geometrical optics and have a pressure contribution as in (1) but with $\beta = 0$. The scattering of sound from fluid [3] or elastic [4,5] spheres gives rise to both focused and unfocused wavefronts as does the scattering of light from bubbles [6,7] and drops [8-10]. In this paper I give new results and note other recent discoveries.

I. WHAT IS THE SHAPE OF THE WAVEFRONT WHICH PRODUCES A TRANSVERSE CUSP CAUSTIC?

The scattering of light from spheroidal drops of water into the rainbow region was recently observed to manifest hyperbolic-umbilic [8,9] and cusp [10] diffraction catastrophes not previously known to appear. The analysis presented here suggests mechanisms for the generation of transverse cusp diffraction catastrophes in acoustics. Figure 1 illustrates what I mean by a transverse cusp. An acoustical or optical wavefront propagates from the (x,y) plane such that a cusp caustic is present in the (u,v) plane which is parallel to the (x,y) plane but is displaced from it by a distance z. The cusp locates the transition in the (u,v) plane of the number of rays which contribute to the amplitude according to geometric optics: point P' is shown in the region where 3 rays contribute whereas outside the cusp only 1 ray contributes. (Of course, as in the scattering from drops [8-10] other rays may be present which do not participate in this catastrophe by merging with the participating rays at the most singular point.) In optics the wave in the exit plane arises from the combined effects of refraction and reflection by a drop while in acoustics the wavefront may be produced by reflection from a curved surface or by a volume perturbation in the speed of sound. It should be emphasized that the cusp considered here differs fundamentally in its orientation (with respect to the wavefront in the exit plane) from the longitudinal cusp in ocean acoustics proposed in unpublished work by R. L. Holford (see Fig. 12.31 of [2]). Holford found that certain depth dependences of the ocean's sound velocity bend rays from a point source upward so as to reflect from the sea surface producing a longitudinal cusp which unfolds along the direction of propagation.

I show here that the wave in the exit plane having a pressure given by the real part of

$$p(x,y) = f(x,y)e^{-i\omega t}e^{ikg}, \quad (2a)$$

$$g(x,y) = a_1x^2 + a_2y^2x + a_3y^2, \quad (2b)$$

produces a transverse cusp. Here $k = \omega/c = 2\pi/\lambda > 0$ where the phase velocity c is constant and the functions f and g are real valued and slowly varying. The Fresnel approximation is used for the distance between representative points P and P' so the analysis is not restricted to the far field. The $\exp(-i\omega t)$ dependence will be suppressed and (to be discussed) f will be taken to be constant and of unit amplitude. The diffracted pressure p(u,v) may then be approximated as

$$p(u,v) = (i\lambda r)^{-1}e^{ikr}F(u,v), \quad (3)$$

$$F = \iint_{-\infty}^{\infty} e^{ik[g + (x^2+y^2)/2z - (xu+yv)/z]}dxdy \quad (4)$$

Introduce the new parameters $b_j = a_j + 1/2z$ and integrate over x. Defining the dimensionless variable $s = y|a_2/2|^{1/2}|k/b_1|^{1/4}$ gives

$$F = |\pi/kb_1|^{1/2}\, e^{\pm i\pi/4} \exp(-iku^2/4b_1z^2)J \qquad (5)$$

$$J(u,v) = |b_1/k|^{1/4}\, |2/a_2|^{1/2} \left\{ \begin{matrix} P^*(X,Y) \\ \\ P(X,Y) \end{matrix} \right\} \qquad (6)$$

where the upper (lower) options in (5) and (6) are used if $b_1 > 0$ ($b_1 < 0$) and P(X,Y) is Pearcey's integral [11,2]

$$P = \int_{-\infty}^{\infty} \exp[i(s^4 + s^2X + sY)]ds; \qquad (7)$$

P* is the complex conjugate. The real parameters X and Y are

$$X = -|k/b_1|^{1/2}[(u/z) + (2b_1b_3/a_2)]\mathrm{sgn}(a_2), \quad (8)$$

$$Y = k^{3/4}\, |b_1|^{1/4}\, |2/a_2|^{1/2}\, (v/z)\mathrm{sgn}(b_1) \qquad (9)$$

The cusp is located at [2,11] $8X^3 + 27Y^2 = 0$ so the cusp point is at $u = 0$ only if $b_3 = 0$. When $a_2 < 0$ the cusp is reversed from the orientation shown in Fig. 1.

For points near the axis the horizontal and vertical observation angles become $\theta \approx u/z$ and $\zeta \approx v/z$. Photographs of optical diffraction patterns which decorate the cusp region are shown in [8,10] and similar distributions in the acoustic intensity are anticipated near a cusp. The Fresnel approximation leading to (3) requires that

$$z^3 >> (1/8)\, k[(x-u)^2 + (y - v)^2]^2, \qquad (10)$$

for (x,y) which contribute significantly to F. The significant (x,y) are near the stationary-phase points of F and for small u and v, (10) becomes $z^3 >> k(b_3^2 + 2b_1b_3)^2/8a_2^4$. It has been assumed that f is slowly varying in the (x,y) region of the stationary phase points of F. Inspection of (3) - (7) shows that $\beta = 1/4$ at the cusp point as has been anticipated [1,2]. For a cusp to be formed it is essential that $a_2 \neq 0$ and $b_1 \neq 0$; when $b_3 = 0$ and $a_2 \rightarrow 0$, $J \rightarrow 2\pi\delta(kv/z)$ as expected.

The wave shape (2b) for generating a transverse cusp appears to be a novel result though it may also be argued from an isomorphism between classes of singularities and Weyl groups and an equivalency relation between the A_3 and D_3 groups. A wavefront of this shape may be produced by reflection from curved surfaces or refraction by inhomogeneities. Note that g is not of the form $ax^4 + bx^2 + cy^2$.

II. OPTICAL GLORY OF BUBBLES IN WATER

When a spherical bubble in a liquid is illuminated, toroidal wavefronts are produced for which $K \rightarrow 0$ in the backward direction. This is an example of an axial caustic [1] for which the scattering amplitude has $\beta = 1/2$. The optical glory of bubbles was first observed for bubbles in an oil [6]; however, it was recently photographed here for freely rising bubbles in water having diameters as large as 0.3 mm. A theory for the optical glory of spherical bubbles in water was confirmed with Mie theory [7]; however, the theory must be modified for bubbles larger than 0.3 mm due to their asphericity. The characteristic backscattering pattern [6,7] may be useful for the remote detection and sizing of bubbles. The forward optical glory of bubbles was also photographed.

III. ACOUSTICAL AXIAL CAUSTICS

When a large elastic sphere is insonified, backward directed toroidal wavefronts are produced as a consequence of bulk transmitted waves [4] and surface waves [5]. The amplitudes for the transmitted-wave glories are characterized by $\beta = 1/2$ though the total steady-state amplitude superposes several classes of waves. The diffraction pattern characteristic of acoustical axial focusing was detected and models for the amplitude were confirmed [4,5]. Models of the acoustical glory of fluid spheres were confirmed by comparison with computations of the partial-wave series [3]. For a particular sound speed ratio β is 2/3 because of a superposition of axial and rainbow-like caustics.

This research was supported by the U.S. Office of Naval Research.

[1] M. V. Berry, Adv. Phys. 25, 1-26 (1976).
[2] T. Poston and I. Stewart, Catastrophe Theory and Its Applications (Pitman, London, 1978).
[3] P. L. Marston and D. S. Langley, J. Acoust. Soc. Am. 73, 1464-1475 (1983); 78, 1128 (1985).
[4] P. L. Marston et al. ibid. 74, 605-618 (1983); 76, 1555-1563 (1984); 78, 1128 (1985).
[5] K. W. Williams and P. L. Marston, ibid. 78, 772-728 (1985).
[6] D. S. Langley and P. L. Marston, Phys. Rev. Lett. 47, 913-916 (1981).
[7] P. L. Marston and D. S. Langley, Proc. SPIE 489, 130-141 (1984).
[8] P. L. Marston and E. H. Trinh, Nature 312, 529-531 (1984).
[9] J. F. Nye, Nature 312, 531-532 (1984).
[10] P. L. Marston, Opt. Lett. 10, 588-590 (1985).
[11] T. Pearcey, Philos. Mag. 37, 311-317 (1946).

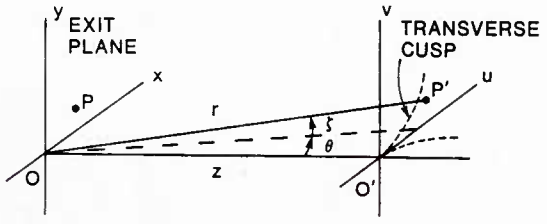

Fig. 1. Diffraction geometry in uniform media.

APRIL 1984

REPORTS DISTRIBUTION LIST FOR ONR PHYSICS DIVISION OFFICE
UNCLASSIFIED CONTRACTS

Director
Defense Advanced Research Projects Agency
Attn: Technical Library
1400 Wilson Blvd.
Arlington, Virginia 22209
1 copy

Office of Naval Research
Physics Division Office (Code 412)
800 North Quincy Street
Arlington, Virginia 22217
2 copies

Office of Naval Research
Director, Technology (Code 200)
800 North Quincy Street
Arlington, Virginia 22217
1 copy

Naval Research Laboratory
Department of the Navy
Attn: Technical Library
Washington, DC 20375
1 copy

Office of the Director of Defense
Research and Engineering
Information Office Library Branch
The Pentagon
Washington, DC 20301
1 copy

U.S. Army Research Office
Box 1211
Research Triangle Park
North Carolina 27709
2 copies

Defense Technical Information Center
Cameron Station
Alexandria, Virginia 22314
12 copies

Director, National Bureau of Standards
Attn: Technical Library
Washington, DC 20234
1 copy

Director
U.S. Army Engineering Research
and Development Laboratories
Attn: Technical Documents Center
Fort Belvoir, Virginia 22060
1 copy

ODDR&E Advisory Group on Electron Devices
201 Varick Street
New York, New York 10014
1 copy

Air Force Office of Scientific Research
Department of the Air Force
Bolling AFB, DC 22209
1 copy

Air Force Weapons Laboratory
Technical Library
Kirtland Air Force Base
Albuquerque, New Mexico 87117
1 copy

Air Force Avionics Laboratory
Air Force Systems Command
Technical Library
Wright-Patterson Air Force Base
Dayton, Ohio 45433
1 copy

Lawrence Livermore Laboratory
Attn: Dr. W. F. Krupke
University of California
P.O. Box 808
Livermore, California 94550
1 copy

Harry Diamond Laboratories
Technical Library
2800 Powder Mill Road
Adelphi, Maryland 20783
1 copy

Naval Air Development Center
Attn: Technical Library
Johnsville
Warminster, Pennsylvania 18974
1 copy

Naval Weapons Center
Technical Library (Code 753)
China Lake, California 93555
1 copy

Naval Underwater Systems Center
Technical Center
New London, Connecticut 06320
1 copy

Commandant of the Marine Corps
Scientific Advisor (Code RD-1)
Washington, DC 20380
1 copy

Naval Ordnance Station
Technical Library
Indian Head, Maryland 20640
1 copy

Naval Postgraduate School
Technical Library (Code 0212)
Monterey, California 93940
1 copy

Naval Missile Center
Technical Library (Code 5632.2)
Point Mugu, California 93010
1 copy

Naval Ordnance Station
Technical Library
Louisville, Kentucky 40214
1 copy

Commanding Officer
Naval Ocean Research & Development Activity
Technical Library
NSTL Station, Mississippi 39529
1 copy

Naval Explosive Ordnance Disposal Facility
Technical Library
Indian Head, Maryland 20640
1 copy

Naval Ocean Systems Center
Technical Library
San Diego, California 92152
1 copy

Naval Surface Weapons Center
Technical Library
Silver Spring, Maryland 20910
1 copy

Naval Ship Research and Development Center
Central Library (Code L42 and L43)
Bethesda, Maryland 20084
1 copy

Naval Avionics Facility
Technical Library
Indianapolis, Indiana 46218
1 copy